Earth-Science Reviews 197 (2019) 102899

Contents lists available at ScienceDirect

Earth-Science Reviews

journal homepage: www.elsevier.com/locate/earscirev

Sources of bias in detrital zircon geochronology: Discordance, concealed lead loss and common lead correction

Tom Andersen[a,b,*], Marlina A. Elburg[b], Boniswa N. Magwaza[b]

[a] Department of Geosciences, University of Oslo, P.O. Box 1047 Blindern, N-0316 Oslo, Norway
[b] Department of Geology, University of Johannesburg, PO Box 524, Auckland Park, Johannesburg 2006, South Africa

ARTICLE INFO

Keywords:
Detrital zircon
U-Pb
Lead loss
Common lead
Lu-Hf
Provenance

ABSTRACT

The distribution pattern of U-Pb ages of detrital zircon in a sedimentary rock is commonly assumed to reflect the ages of igneous or metamorphic processes in rocks that have contributed material to the sedimentary basin (i.e. the protosources), directly or through recycling of older sedimentary rocks. If the Pb isotopic composition of detrital zircon is modified by processes after crystallization, or influenced by unintended effects of data treatment such as discordance filters and common lead correction, the value of detrital zircon as geological indicator is compromised. Discordance filters will identify zircons having suffered recent lead loss, but significant amounts of ancient lead loss may pass undetected. Lead loss events after the zircon's primary crystallization can be induced by regional or contact metamorphism, but also by low temperature processes during diagenesis and weathering, and can be coupled to uptake of a mixture of common lead and unsupported radiogenic lead, which cannot be properly corrected by common-lead correction routines. Concealed ancient lead loss and over-correction for common ^{207}Pb may cause bias towards lower ages, while remaining within acceptable discordance limits. This creates spurious age fractions that may give false indications of sedimentary provenance, invalidate estimates of maximum limits for the age of deposition, and cause problems for comparison and correlation studies based on detrital zircon age data. Careful scrutiny of all U-Pb analyses in combination with Hf isotope analysis may help identifying these effects in detrital zircon data, but will not provide a universal guarantee against biased age spectra.

1. Introduction

U-Pb age data from detrital zircons in clastic sedimentary rocks have become a standard tool to identify provenance of detritus, to compare and correlate successions, and to define limits for the age of deposition (e.g. Gehrels, 2014; Zimmermann, 2018 and references therein). The age of a detrital zircon reflects the age of a zircon-forming, igneous or metamorphic event in a source rock (the *protosource*), from which the zircon has made its way to the site of final deposition through one or more erosion – transport – deposition cycles. A detrital zircon *population* (Andersen et al., 2018a) comprises all zircons in the sediment or sedimentary rock sampled, the properties of which must be estimated from analytical data on a much smaller number of zircon grains analysed. Such a detrital zircon data set, and by inference the detrital zircon population of the sediment as a whole, can be subdivided into fractions based on some pre-defined criteria, for example *age fractions* that are constrained by upper and lower age limits. The rationale behind this nomenclature has been explained elsewhere (Andersen et al., 2018b).

Much effort has been put into development of in-situ methods of U-Pb and Lu-Hf isotope analysis by SIMS (secondary ion mass spectrometry) and LA-ICPMS (laser ablation inductively coupled plasma source mass spectrometry), and tools to handle detrital zircon data (e.g. Sambridge and Compston, 1994; Williams, 1998; Sircombe, 2000; Vermeesch, 2013, 2018; Satkoski et al., 2013; Eizenhöfer et al., 2015; Andersen et al., 2018b). Provided that the best available analytical protocols and standardization routines are used in the laboratory, the main source of uncertainty in a detrital zircon age distribution is not the analytical uncertainty from the mass spectrometer, but the statistical error associated with the random sampling of zircon grains for analysis, which, for realistic numbers of analyses, leads to relatively wide simultaneous confidence intervals (i.e. confidence bands, e.g. Wassermann, 2006) around cumulative age distribution curves (Andersen, 2005; Andersen et al., 2016a, 2018b).

The issue of *accuracy* of detrital zircon distributions has received much less attention. It remains a basic, implicit or explicit, assumption in such studies that the age distribution pattern of detrital zircon in a

* Corresponding author at: Department of Geosciences, University of Oslo, Norway.
E-mail address: tom.andersen@geo.uio.no (T. Andersen).

https://doi.org/10.1016/j.earscirev.2019.102899
Received 27 February 2019; Received in revised form 24 June 2019; Accepted 12 July 2019
Available online 17 July 2019

sediment gives a representation of the geological history of the protosource terrane(s) in which *no geologically significant age fractions are systematically overlooked, and no spurious age fractions are introduced*, which will here be referred to as *"the assumption of qualitative representativity"*. A detrital zircon age distribution pattern may be said to be *biased* when this assumption is violated so that age fractions in the protosource(s) are either systematically removed or shifted in age, spurious age fractions are introduced, or their relative abundances are changed beyond the confidence limits of distribution curves. Because this review is concentrating on detrital zircon in Palaeoproterozoic rocks, the ages considered are $^{207}Pb/^{206}Pb$ ages, unless otherwise stated. Applications of detrital zircon age data that implicitly or explicitly assume qualitative representativity include identification of protosources, comparison between samples, correlations within or between basins, and the use of "the youngest detrital zircon" or "youngest significant age fraction" to define a maximum age of deposition of the host sediment. All of these applications may be compromised by bias.

The aim of this study is to identify some sources of potential bias in detrital zircon age distribution patterns that can be related to the U-Pb systematics of zircon and the methods used to handle analytical data. The effects are illustrated by an examination of several published datasets with a focus on clastic sedimentary rocks from southern Africa, mainly of Palaeoproterozoic age, and some additional data that are presented here (Supplementary Table S1). Potential consequences for the application of detrital zircon data to geological problems are discussed. The purpose is not to challenge the interpretations of the authors of the original studies, but to explore the limits of accuracy in current detrital zircon geochronology. Systematic errors due to poor calibration or analytical artifacts in the mass spectrometer laboratory will not be considered here, nor will age fractionation due to selective removal of radiation damaged zircon during transport (e.g. Markwitz and Kirkland, 2018) or sample preparation (e.g. Sircombe and Stern, 2002). When working with detrital zircons, it is important also to realize that the only protosources that can be detected are zircon-bearing rocks (e.g. felsic, igneous rocks). Rocks devoid of zircon (e.g. many mafic and ultramafic rocks) may have contributed detritus to a sedimentary basin, but such protosources cannot be detected from detrital zircons. This is a self-evident limitation of the detrital zircon approach to provenance analysis that will not be further considered here. There are, however, other methods that can be applied (heavy mineral studies, whole-rock trace element geochemistry and Nd isotopes).

2. Discordant zircons and effects of lead loss

Absolute concordance of $^{207}Pb/^{235}U$ and $^{206}Pb/^{238}U$ ages (i.e. a zircon plotting exactly on the concordia curve, as illustrated by point *a* in Fig. 1) is uncommon. A zircon plotting below the concordia curve in a $^{206}Pb/^{238}U$ vs. $^{207}Pb/^{235}U$ diagram (i.e. the conventional concordia diagram) by more than analytical uncertainty is said to be normally discordant. In this paper, discordance is defined from isotope ratios rather than ages. For point *c* in Fig. 1, the discordance (in percent) is defined by *(co/ao-1)*100* where *co* is the length of the line segment between the observed point and the origin, and *ao* is the length of the line through the point from its intersection with the concordia at *a* to the origin. Defined in this way, normal discordance is given as a negative percentage. For zircons from magmatic rocks, it is in principle possible to define a discordia line and its upper intercept with the concordia (i.e. the true crystallization age) by linear regression of analyses showing variable degrees of discordance. For detrital zircon, this is in general not possible (but see Nemchin and Cawood, 2006), and care must be taken to define criteria to distinguish between grains that convey useful information from those that have been too severely disturbed to do so.

There are in principle three processes that can induce normal discordance in zircon: (i) Loss of radiogenic lead and (ii) Gain of excess uranium after primary crystallization, or (iii) Incorporation of common lead (Section 3, below). Lead loss and U-gain act along a discordia line connecting the primary crystallization age on the concordia (i.e. the upper intercept) to a lower concordia intercept representing the age of disturbance of the U-Pb system. A fourth mechanism, which will not be considered here, is an artifact in the laboratory due to accidental mixing of material from concordant domains with distinct ages, which will produce points along a mixing line (e.g. Mezger and Krogstad, 1997). This is mainly a problem for methods in which whole grains are dissolved and homogenized, but less so in time-resolved analysis using microbeam instruments, which allow such heterogeneities to be detected during data reduction.

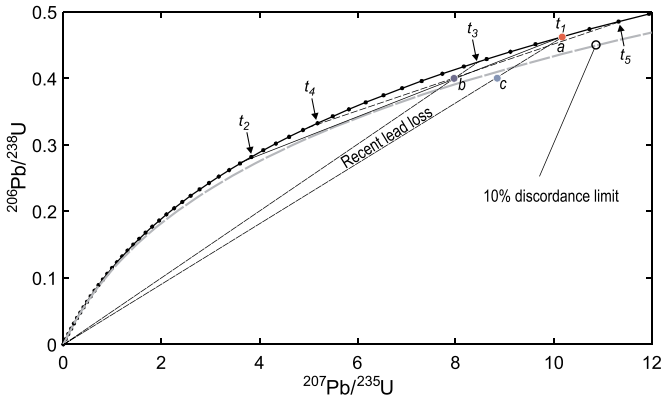

Fig. 1. A theoretical example showing how ancient lead loss may escape detection by a data filter based on a discordance limit. See Section 2.1 in the text for explanation, and Section 5.2 for a discussion of implications for estimates of the maximum age of deposition made from detrital zircon ages.

Loss of radiogenic lead in zircon is commonly attributed to metamorphic overprint or to interaction with aqueous fluid (e.g. Rubatto, 2017, and references therein). Since a remarkable study by Williams (2001), in which it was demonstrated that the U-Pb system of detrital zircon in a suite of high-grade metasedimentary rocks remained undisturbed even at anatectic grade, the possibility of ancient, post-depositional lead loss has generally been disregarded in the interpretation of detrital zircon age distributions. However, some studies have demonstrated effects of lead-loss after deposition induced by diagenetic fluids (Willner et al., 2003), by regional metamorphism (Orejana et al., 2015) or contact metamorphism (Andersen, 2013; Zeh et al., 2016). Whereas fully crystalline zircon is in general resistant against alteration during chemical weathering, zircon that has suffered radiation damage is reactive, and significant element mobility and redistribution of both uranium and lead within crystals and between zircon grains and their surroundings may take place, especially under tropical weathering conditions (e.g. Stern et al., 1966; Balan et al., 2001; Delattre et al., 2007; Pidgeon et al., 2013, 2017; Kielman et al., 2018). In the oxidizing environment of a modern, near-surface weathering zone, uranium is mobile as the soluble UO_2^{2+} complex ion. Hexavalent uranium can only enter crystalline zircon if reduced, but it may be absorbed into metamict domains, or precipitated as submicroscopic, secondary uranyl minerals, for example along fractures in the altered zircon. The presence of such secondary uranyl minerals can be detected by methods such as backscattered electron imaging or X-ray mapping in a scanning electron microscope or an electron microprobe, neither of which are in common use in detrital zircon studies.

2.1. Discordance limits and concealed lead loss

Whereas more sophisticated methods have been proposed (e.g. Nemchin and Cawood, 2006; Reimink et al., 2016), the most common approach to the discordance problem is to exclude points that fall outside an envelope around the concordia curve, defined by, for

Table 1
Samples reviewed in this study.

	Lat (Deg. S)	Long (deg. E)	Rock type	^{N}U-Pb	^{N}Lu-Hf	Sample type	Method	Reference
Magaliesberg formation								
Mag-R1	26.7798	27.2581	Quartzite	101	97	Single sample	LA-ICPMS	Zeh et al. (2016)
BQz-1	24.3050	30.0033	Quartzite	98	98	Single sample	LA-ICPMS	Zeh et al. (2016)
BQz2	24.3059	30.0047	Quartzite	118	110	Single sample	LA-ICPMS	Zeh et al. (2016)
BQz3	24.3062	30.0052	Quartzite	99	99	Single sample	LA-ICPMS	Zeh et al. (2016)
BQz5	24.3036	30.1765	Quartzite	58	41	Single sample	LA-ICPMS	Zeh et al. (2016)
CH7	24.4642	30.1391	Quartzite	113	110	Single sample	LA-ICPMS	Zeh et al. (2016)
JF8	24.5495	29.8512	Quartzite	143	102	Single sample	LA-ICPMS	Zeh et al. (2016)
MEMG3[a]	24.3142	30.0287	Quartzite	75	69	Single sample	LA-ICPMS	This work
MEMG4[a]	24.3061	30.0047	Quartzite	98	69	Single sample	LA-ICPMS	This work
MAG	25.8667	27.5000	Quartzite	29	0	Composite over 200 stratigraphic metres	SIMS	Schröder et al. (2016)
Makganyene formation								
MPT-4	28.5667	22.8833	Diamictite	61	0	Drillcore sample	SIMS	Moore et al. (2012)
Kuruman formation								
CN111	27.1844	23.0860	Mudstones	137	0	Drillcore samples (pooled)	SIMS	Pickard (2003)
CN118	27.1844	23.0860	Mudstones	86	0	Drillcore samples (pooled)	SIMS	Pickard (2003)
Waterberg group								
SA16–402	24.2462	27.9661	Sandstone	52	52	Single sample	LA-ICPMS	Andersen et al. (2019)
Natal group (Ordovician)								
SA12/20	29.8058	30.8039	Sandstone	87	87	Single sample	LA-ICPMS	Kristoffersen et al. (2016)

[a] Data in Supplementary Table S1.

example, 5% or 10% discordance (e.g. Moore et al., 2012; Zeh et al., 2016). Discordance can be reported for the observed $^{207}Pb/^{235}U$ and $^{206}Pb/^{238}U$, i.e. for the centre of its error ellipse relative to the concordia along a straight line from the origin through the observed point to interception with the concordia ("central discordance"), or for the point on the perimeter of a 1σ, 2σ or 95% confidence error ellipse that most closely approaches the concordia ("minimum rim discordance"). When applying a constant discordance filter, it is commonly applied to the observed, central discordance, which means that analytical errors are not explicitly considered. This is permissible as long as the discordance limit used (e.g. 10%) exceeds the analytical error of the individual point (commonly 1–2%). Effects of analytical uncertainty will be reviewed separately in Section 2.3, below.

A simple illustration of how lead loss can cause age bias that remains hidden in data that pass a discordance filter, and which would therefore be assumed to retain qualitative representativity, is shown in Fig. 1. Three detrital zircon grains (*a, b, c*) have been separated from a sedimentary rock of unknown age. Grain *a* plots exactly on the concordia curve at t_1, which can be taken as a robust estimate of its crystallization (i.e. protosource) age. Grain *c* gives the same $^{207}Pb/^{206}Pb$ age, but plots outside of the 10% discordance limit and would therefore be rejected from the age distribution, although the $^{207}Pb/^{206}Pb$ age still represents its true crystallization age as long as lead loss took place only at $t = 0$. Zircon grain *b* is weakly discordant, but plots within the 10% discordance envelope, and would therefore be accepted as part of a valid age distribution at its $^{207}Pb/^{206}Pb$ age (t_3), implicitly assuming that the minor degree of discordance observed is due only to recent lead loss. However, this may not necessarily be the true age of the zircon, which could have a more complex history: it could have been generated from a concordant zircon of age t_1 by partial lead loss at t_2, from an older grain of age t_5 by lead loss at t_4, or in fact by any combination of upper- and lower intercept ages and degrees of lead loss that bring a point inside of the 10% discordance envelope.

Zircon grains that have been affected by an ancient lead loss event, and yet remain within acceptable discordance limits have suffered *concealed lead loss*. The age of such zircons will not reflect the crystallization age of the protosource. Concealed lead loss can take place prior to final deposition (e.g. by weathering or metamorphism of the protosource rock or a sedimentary precursor), or after deposition of the host sediment. The overall effect of concealed, partial lead loss on a suite of zircons (detrital or otherwise) is likely to be a random distribution of $^{207}Pb/^{206}Pb$ ages that is difficult to relate to some defined geological process, or in the case of detrital zircons, to an identifiable source terrane.

2.2. An example: the Magaliesberg quartzite

The Palaeoproterozoic Magaliesberg Formation of the Pretoria Group in South Africa consists of quartz arenite deposited on Kaapvaal Craton basement; it was intruded, and locally contact metamorphosed by the 2055 Ma Bushveld complex (Eriksson et al., 2006; Cawthorn et al., 2006; Zeh et al., 2015, 2016). Pertinent information on detrital zircon samples from the formation (location, rock type, number of grains analysed, methods used, for the published data as well as for samples analysed in this study) is given in Table 1.

Detrital zircon data of a composite sample (MAG, Table 1) collected in a 200 m stratigraphic section through the Magaliesberg Formation in its type area were published by Schröder et al. (2016) based on SIMS U-Pb analyses by Dorland (2004). Zeh et al. (2016) published U-Pb and Hf isotope analyses by LA-ICPMS on seven samples of recrystallized quartzite from localities within the contact aureole of the Bushveld intrusion. U-Pb and Lu-Hf data on two additional samples of recrystallized Magaliesberg Formation quartzite, also from within the Bushveld contact aureole (MEMG3 and MEMG4, see Table 1), are given in Supplementary Table S1. Information on the analytical methods used in this study is given in Appendix 1 (electronic supplement). Samples BQz2, BQz3 (Zeh et al., 2016) and MEMG4 (this study) were taken from a ca. 60 m section in a continuous roadcut exposure of Magaliesberg quartzite, although the three samples may come from different beds within the formation.

The complete set of detrital zircon U-Pb data from the Magaliesberg Formation is plotted in Fig. 2. All samples contain a significant age fraction in the range 2200–2300 Ma and subordinate age fractions in the Archaean, with a large proportion of discordant grains falling outside of the envelope defined by a ± 5% discordance limit used by Zeh et al. (2016) (Fig. 2a, b). This also applies to the new samples MEMG3 and MEMG4 (for background information on these samples, see Table 1), with the main difference between the two samples being a larger proportion of Archaean zircon in MEMG3 (Fig. 2c). Zircons younger than ca. 2200 Ma were not reported in the smaller SIMS dataset published by Schröder et al. (2016) (Fig. 2b). All other samples contain "tails" of younger zircons, most of which are discordant,

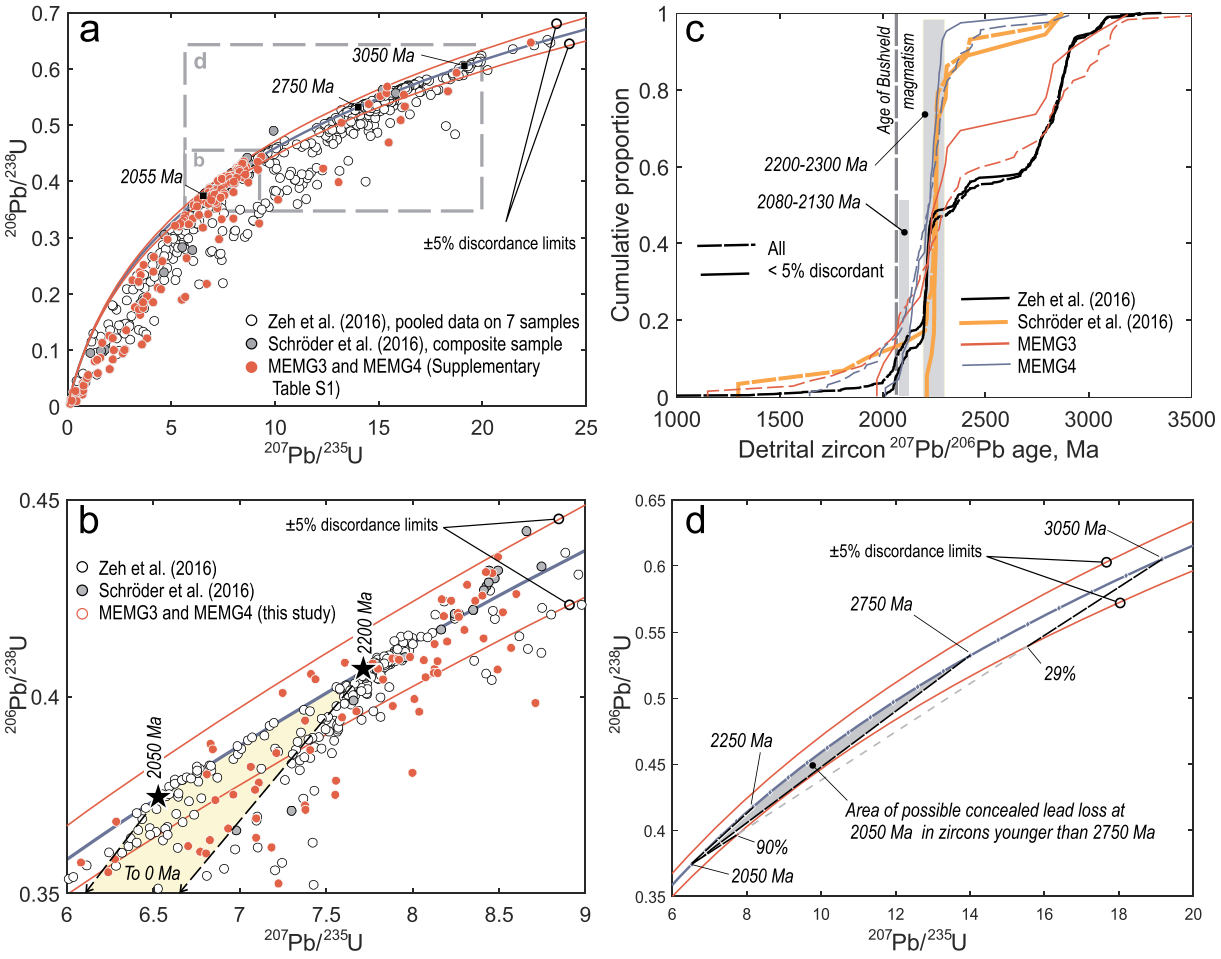

Fig. 2. The complete set of U-Pb data on detrital zircon in the Palaeoproterozoic Magaliesberg Formation quartzite, South Africa. For sources of data, sample coordinates and number of grains analysed, see Table 1. Data on all seven samples from Zeh et al. (2016) have been pooled in this figure ($\Sigma N = 730$). Common lead corrections as in the original papers and for samples MEMG3 and MEMG4 as given in Supplementary Table S1; for background information on these samples, see Table 1.

a: The complete dataset, including concordant and discordant zircon. The discordance limits of ± 5% used by Zeh et al. (2016) are indicated.

b: Detail of *a* in the age range 2000–2400 Ma. Any 2050 Ma to 2200 Ma grains that have lost lead at the present day will plot within the shaded sector, which continues to the origin. Discordance limits of ± 5% are indicated.

c: Empirical cumulative distribution curves for detrital zircon ages in the three sets of data from the Magaliesberg Formation with all analysed grains included (dashed curves) and data filtered at a 5% discordance limit (solid curves).

d: Part of the concordia diagram (drawn to scale) to illustrate the possibility of ancient, post-depositional lead loss to remain concealed within ± 5% discordance limits. Zircons that were concordant at an age younger than 2750 Ma will remain within the ± 5% discordance limits at any degree of lead loss at 2050 Ma (shaded field limited by the concordia and the discordia line from 2750 Ma to 2050 Ma). A 3050 Ma zircon losing lead at 2050 Ma can suffer 29% of lead loss before leaving the envelope defined by the discordance limits, and will re-enter at ≥90% lead loss.

extending to ages younger than the minimum possible depositional age defined by the 2055 Ma emplacement age of the Bushveld complex (Fig. 2c).

Sample BQz3 of Zeh et al. (2016) contains a distinct fraction of concordant and near-concordant zircons at 2080–2130 Ma, which is scarce or absent in the other samples from the Magaliesberg Formation, including samples BQz2 and MEMG4. Zeh et al. (2016) reported evidence of new growth and recrystallization of zircon at the time of emplacement of the Bushveld complex and later, but regarded zircons in the range 2080–2130 Ma age range, with intact oscillatory zoning patterns and < 5% discordance as representing protosource ages.

Even within the rather narrow 5% discordance envelope, any concordant zircon formed in protosources younger than ca. 2750 Ma will stay within the concordance envelope at all degrees of lead loss that could be induced by the Bushveld magmas at 2055 Ma (shaded section in Fig. 2d). Zircon grains older than this limit (e.g. the 3050 Ma example shown in Fig. 2d) may also suffer non-trivial amounts of lead loss (≤29%) before leaving the envelope, and will re-enter the envelope at very high degrees of lead loss (≥90%). The consequence of this is that significant shifts towards younger $^{207}Pb/^{206}Pb$ ages than the true protosource age are possible, even for zircons that remain within the 5% discordance limit relative to the concordia, and this includes zircons of the 2080–2130 Ma age fraction. Hf isotope data from the Magaliesberg Formation will be considered in Section 4, below.

2.3. Correlated analytical errors, lead loss and false concordance

Measured $^{206}Pb/^{238}U$ and $^{207}Pb/^{235}U$ ratios typically have analytical uncertainties that are positively correlated, because of the constant $^{235}U/^{238}U$ ratio in nature (Gale, 1979; Ludwig, 2012). U-Pb ages of individual zircon grains analysed by microbeam methods are commonly reported with 2σ or 95% confidence uncertainty in the order of 1–2%, with correlation coefficients (ρ) in the range 0.7–0.98. A consequence of the positive error correlation is that the major axis of the error ellipse around a point in a conventional concordia diagram will have a positive slope.

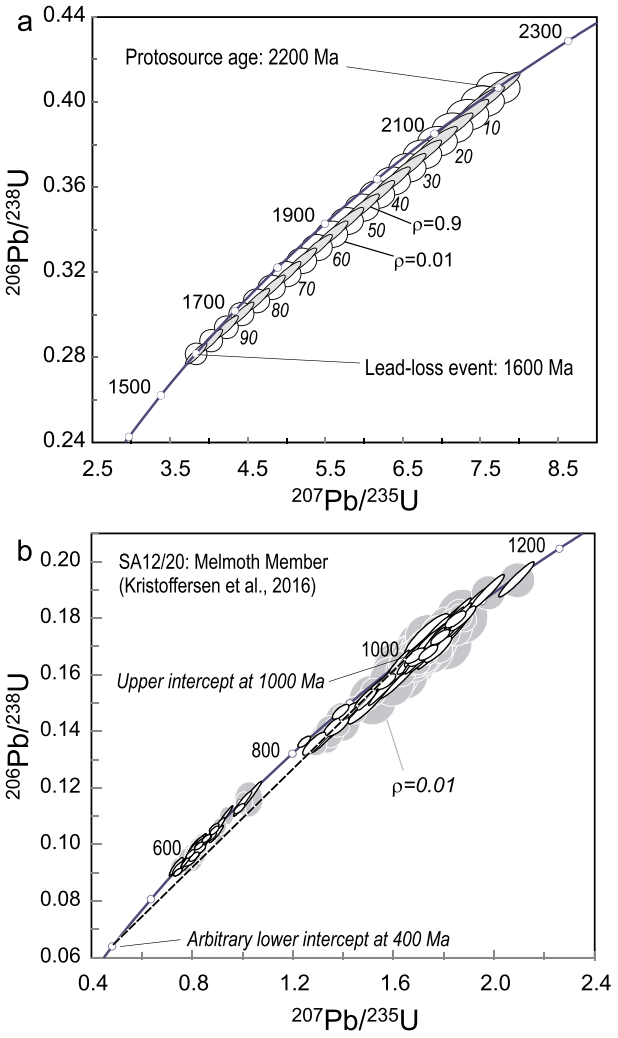

Fig. 3. Effects of error correlation on U-Pb discordance.
a: A simple example of lead loss at 1600 Ma affecting zircon with a uniform age of 2200 Ma whose $^{206}Pb/^{238}U$ and $^{207}Pb/^{235}U$ ratios have been measured with relative 1σ errors of 0.75 and 1.5%, respectively. Points are shown at intervals of 5% lead loss. The grey ellipses are constructed with an error correlation coefficient $\rho = 0.9$, the white with $\rho = 0.01$, i.e. practically uncorrelated errors. b: Data for a sample of the Melmoth Member, Durban Formation, Natal Group (KwaZulu-Natal, South Africa) from Kristoffersen et al. (2016) shown with the observed error correlation coefficients (white ellipses) on a shaded background of the same data plotted with $\rho = 0.01$. The data set comprises 112 analyses (Table 1). The dashed line is a discordia line from 1000 Ma to 400 Ma, illustrating the effects of lead loss after deposition of the host sediment (e.g. during diagenesis). For background information on the sample, see Table 1.

The curvature of the concordia in a $^{206}Pb/^{238}U$ vs. $^{207}Pb/^{235}U$ diagram is such that the distance between a discordia line and the concordia itself will increase with increasing degree of lead loss, but decrease again at high degrees of lead loss nearing the lower intercept point (Fig. 3a). A point whose uncertainty ellipse intersects the concordia is in principle concordant within analytical uncertainty. This is in general a stronger concordance criterion than that provided by a constant discordance limit as in Fig. 2a, b, d. Nevertheless, grains that have suffered significant amounts of lead loss may appear concordant within analytical uncertainty at ages lower than their true crystallization age. This "sliding along the concordia" effect in microbeam U-Pb data has been recognized at least since the work of Knudsen et al. (1997), and may create anomalously young but apparently concordant zircon ages.

The extent to which the error ellipse around a point in the diagram intersects the concordia depends on the error correlation. A simple example is shown in Fig. 3a, assuming that concordant zircons of uniform age from a 2200 Ma protosource have suffered variable degrees of lead loss at 1600 Ma. For 1σ errors of 0.75 and 1.5% in the $^{206}Pb/^{238}U$ and $^{207}Pb/^{235}U$ ratios, respectively, grains that have suffered less than 20% of lead loss will remain formally concordant at $\rho = 0.9$, and the entire range from zero to 100% lead loss will appear formally concordant at ρ close to zero. Despite of the inherently high error correlations in U-Pb data, underestimating ρ is a realistic problem when using data reduction software that ratios average Pb and U isotope measurements, rather than the average of ratios (e.g. Vorster et al., 2016).

2.4. An example: the Natal Group, South Africa

An illustration of the effect of the error correlation coefficient in a real dataset is given in Fig. 3b, showing data from a sample from the Ordovician Natal Group in KwaZulu-Natal, South Africa (Kristoffersen et al., 2016). The data have been filtered at 10% normal discordance. The data are plotted at the observed error correlations ($\rho = 0.59–0.98$) on a background defined by the same points, but with uncorrelated errors ($\rho = 0.01$). The Natal Group in general shows age fractions in the range 950–1150 Ma and 600–700 Ma, and a scarcity of points in the range 700 to ca. 950 Ma (Kristoffersen et al., 2016). Concordant grains in the sample shown in Fig. 3b cluster in the latest Mesoproterozoic and the late Neoproterozoic, with only two out of 87 grains giving formally concordant ages between 900 Ma and 700 Ma, in agreement with the general age distribution pattern of the Natal Group. Using the observed error correlations, the older of the clusters has a "tail" of grains that are weakly discordant at the 2σ confidence level, with $^{206}Pb/^{238}U$ ages extending down to 800 Ma. This trend can, for example, be a result of lead loss induced by diagenetic fluids after deposition, as tentatively indicated by the dotted discordia line to an arbitrary 400 Ma lower intercept. If the error correlations are disregarded, grains plotting along this weakly discordant "tail" will appear as formally concordant at the ± 2σ level, and the age range of the older cluster of concordant grains will extend to ca. 800 Ma, thus significantly reducing the gap between the two fractions reported by Kristoffersen et al. (2016).

3. Effect of common lead correction

Common lead in a zircon is lead that is not supported by uranium in the crystal structure, including the non-radiogenic isotope ^{204}Pb (Williams, 1998; Andersen, 2002 and references therein). The ionic radius of Pb^{2+} (1.43 Å; Shannon, 1976) is too large to fit into the 8-coordinated positions in the zircon structure occupied by Zr^{4+} (0.98 Å) and substituents such as Hf^{4+} (0.97 Å) or U^{4+} (1.14 Å). Nevertheless, detectable amounts of common lead are frequently encountered in zircon U-Pb geochronology. Although trace amounts of common lead may have been incorporated at the time of crystallization, more important causes for the presence of common lead are processes during weathering or hydrothermal alteration, especially when affecting radiation-damaged crystals (Black, 1987; Pidgeon et al., 2017). Furthermore, unsupported lead in microbeam analyses may originate from the mounting medium, from the sample surface or from cracks formed during sample preparation, and in SIMS analyses also from the gold coating applied (Williams, 1998). Although unrelated to the zircon itself, such lead cannot be distinguished from common lead hosted in the crystal, and is therefore treated by the same correction methods.

3.1. Methods for common lead correction

Correction for common lead involves the solution of a mass balance problem with two or three components (concordant radiogenic lead, common lead and a possible, isotopically indifferent" lead-loss" component; Andersen, 2002). There are at least four different approaches to

common lead correction in use.

3.1.1. The 204-correction

The 204-correction is the traditional, and in general most robust method available (e.g. Williams, 1998). The $^{206}Pb/^{204}Pb$ ratio of the zircon (or its inverse) is measured, and corresponding amounts of ^{206}Pb, ^{207}Pb and ^{208}Pb are subtracted from the raw data, based on assumed $^{206}Pb/^{204}Pb$, $^{207}Pb/^{204}Pb$ and $^{208}Pb/^{204}Pb$ ratios of common lead. $^{204}Pb/^{206}Pb$ of a corrected zircon is zero, and it may be concordant or normally discordant in $^{206}Pb/^{238}U$ and $^{207}Pb/^{235}U$ (Fig. 4a). Reverse discordance in 204-corrected U-Pb data is an indication that the 204 content of the zircon has been overestimated (e.g. due to unresolved interference from ^{204}Hg in LA-ICPMS analysis), or the use of too high $^{206}Pb/^{204}Pb$ and $^{207}Pb/^{204}Pb$ ratios for common lead, or that more complex processes than combined lead loss and common lead incorporation have been involved (e.g. Williams et al., 1984; Kusiak et al., 2013; Ge et al., 2018).

3.1.2. The 207- and 208-corrections

The 207-correction (Williams, 1998; Ludwig, 2012) assumes that the observed lead composition is a true binary mixture of concordant radiogenic lead and common lead, i.e. that the zircon has not suffered any lead loss after its initial crystallization. In a conventional concordia diagram, this correction method amounts to projecting from the observed composition to the concordia along a mixing line whose slope is given by the $^{206}Pb/^{207}Pb$ ratio of common lead (Fig. 4a). Therefore, 207-corrected zircons are always concordant, and give the true age (i.e. the age of crystallization in the protosource) *only* when the zircon is unaffected by lead loss after crystallization of the protosource. Zircon grains that have lost lead at any time of their history will give 207-corrected ages that are too young. The 207-correction has been applied to detrital zircon data by e.g. Pease and Scott (2009), Beranek et al. (2013) and Haines et al. (2013).

A *208-correction* working along similar lines has also been proposed (Ludwig, 2012), assuming the radiogenic lead component to be concordant in $^{208}Pb/^{232}Th$ and $^{206}Pb/^{238}U$, while potentially discordant in its $^{207}Pb/^{235}U$ and $^{206}Pb/^{238}U$ ratios. This is a highly unlikely scenario, and radiogenic lead that is not concordant in all three ratios is likely to give erratic ages when corrected this way. The authors know of no example of this method being applied to detrital zircon data.

3.1.3. Modelling of the 3D discordance pattern without knowledge of ^{204}Pb

If the age of a potential lead-loss event is known or can be estimated with some confidence, it is in principle possible to solve the three-component mass balance problem of common-lead contaminated zircon which has also suffered lead loss without knowledge of the $^{206}Pb/^{204}Pb$ ratio of the zircon (Andersen, 2002). Precise measurement of the four ratios $^{206}Pb/^{238}U$, $^{207}Pb/^{235}U$, $^{208}Pb/^{232}Th$ and $^{232}Th/^{238}U$ is required, as is knowledge of the composition of common lead. The main source of systematic error in zircons corrected this way is the age of lead loss, a false assumption of which may cause severe bias either way in the corrected data. Furthermore, correction of zircons that have lost more than ca. 5% of their radiogenic lead is likely to suffer from systematic errors. For further discussion of bias induced by this method, see Andersen (2002). The method was developed as a last-resort approach to be applied in situations where ^{204}Pb cannot be determined with any degree of confidence, e.g. because of severe Hg contamination in LA-ICPMS analysis. In all other situations, the 204-correction will give more robust results, even when the $^{206}Pb/^{204}Pb$ ratio has elevated uncertainty. For moderately high levels of Hg contamination, the use of a gold trap in the gas supply line may reduce the Hg level sufficiently to allow the ^{204}Pb correction to be used (e.g. Storey et al., 2006).

3.1.4. The Tera-Wasserburg concordia diagram

In a $^{207}Pb/^{206}Pb$ vs. $^{238}U/^{206}Pb$ diagram (Tera and Wasserburg, 1972), two-component mixtures with variable proportions of radiogenic lead of a constant age and common lead of constant composition define a mixing line between the radiogenic lead composition on the concordia curve and common lead at the intersection with the $^{207}Pb/^{206}Pb$ axis (Fig. 4b). Similar to a conventional isochron diagram (e.g. Rb-Sr) this method yields both an age (defined by the concordia intercept of the mixing line) and an "initial ratio", i.e. the $^{207}Pb/^{206}Pb$ of common lead. The approach has been used with success in LA-ICPMS U-Pb dating of magmatic, high-common lead minerals such as perovskite (e.g. Batumike et al., 2008), but is less likely to give useful results for detrital zircons, which are unlikely to have a uniform age, and therefore will show spread in the diagram rather than concentration around a line. Loss of radiogenic lead will cause points to shift from the mixing line towards higher $^{238}U/^{206}Pb$ ratios, along lines whose slopes reflect the age of lead loss (Fig. 4b); if lead loss is recent, the slope of the line is horizontal. Lead loss thus causes additional spread in the diagram that severely reduces the usefulness of this correction method for detrital zircon data.

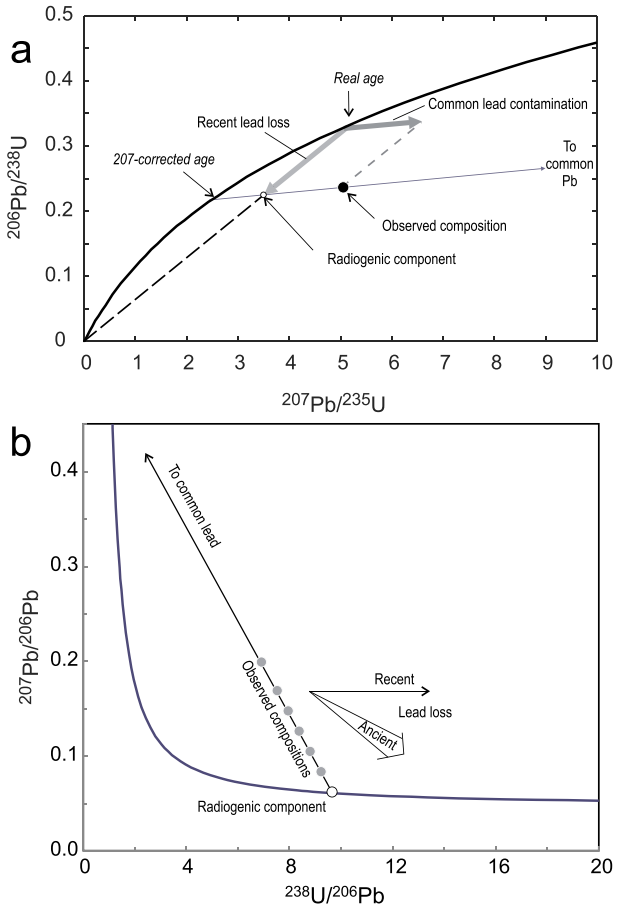

Fig. 4. Principles of common lead correction.
a: The observed composition (black point) is normally discordant due to a combination of recent lead loss (pale grey arrow) and contamination with common lead (darker arrow). The radiogenic lead component should plot on the discordia line from the real age to the origin (white circle), and it is the aim of a common lead correction to remove the excess ^{207}Pb and ^{206}Pb due to common lead to reproduce this point. A ^{207}Pb-correction will remove an excessive amount of common lead to bring the corrected point to the concordia curve.
b: A general illustration of how common lead-bearing zircons of uniform age can be plotted in a Tera-Wasserburg concordia diagram to simultaneously determine age and common lead composition. See Section 3.1.4 in the text for further explanation.

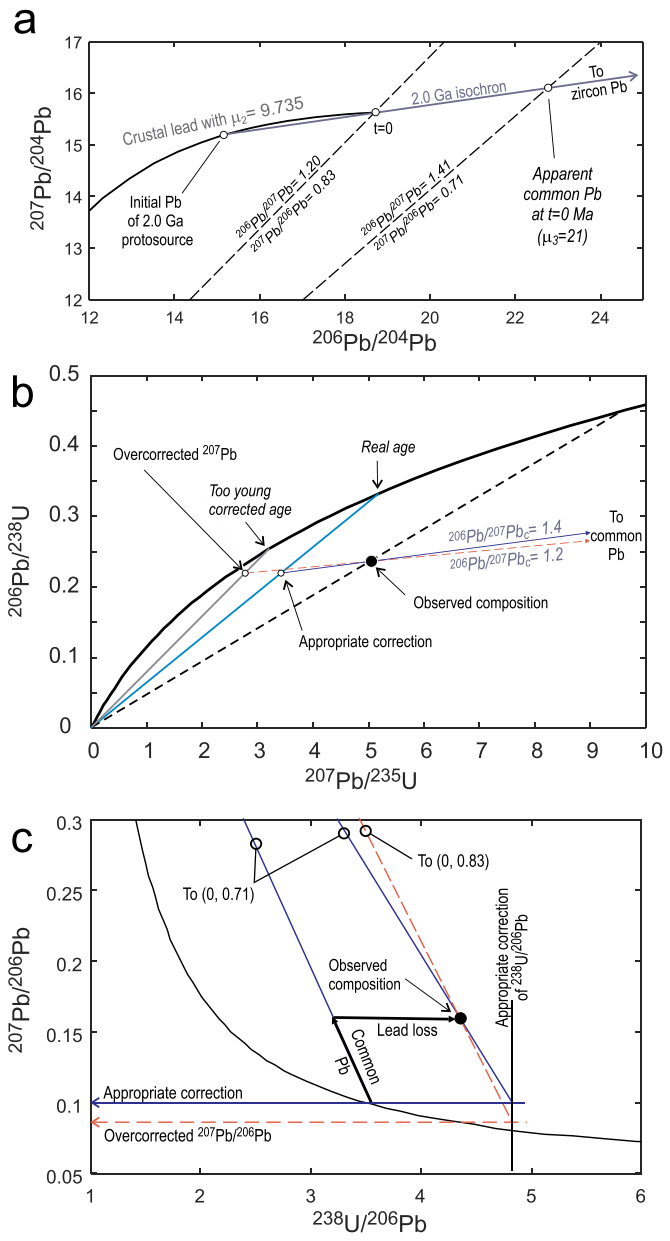

Fig. 5. Effect of common lead composition on common lead correction.
a: Evolution of average crustal lead according to the model of Stacey and Kramers (1975), with initial lead of systems isolated at 2.0 Ga, and zero indicated. At the present day, 2.0 Ga zircon with $\mu_3 >> 9.735$ will plot at a point on the 2.0 Ga isochron line far off scale of the diagram. During recent weathering, zircons interact with lead containing a mixture of the initial lead of the system released from U-free minerals, and radiogenic lead released from zircon. Common lead compositions with the average composition of modern continental crust ($^{206}Pb/^{207}Pb$ = 1.20, $^{207}Pb/^{206}Pb$ = 0.83) and with apparent μ_3 = 21 are shown ($^{206}Pb/^{207}Pb$ = 1.41, $^{207}Pb/^{206}Pb$ = 0.71). For a general introduction to the Pb isotope systematics of multi-stage systems, see e.g. Halla (2018).
b: Effect of common lead correction of zircon that has incorporated common lead during recent weathering, using an inappropriate common lead composition ($^{206}Pb/^{207}Pb$ = 1.20) and one that accounts for the more radiogenic lead composition encountered by the zircon in the process. See Section 3.2 in the text for further explanation.
c: The effect of common lead composition illustrated in a Tera-Wasserburg concordia diagram. Note that the compositions of common lead are now situated at points on the $^{207}Pb/^{206}Pb$ axis, rather than at infinity as in (b). Choice of an average, crustal common lead composition ($^{207}Pb/^{206}Pb$ = 0.83, i.e. $^{206}Pb/^{207}Pb$ = 1.21) causes a significant underestimate of the $^{207}Pb/^{207}Pb$ ratio of the corrected grain, and hence of the $^{207}Pb/^{206}Pb$ age of the zircon. In this example, the overcorrected age (1338 Ma) underestimates the true age (1624 Ma) by 286 Ma.

3.2. The composition of common lead

Common to three of the four common lead correction methods outlined above is the need of prior knowledge of the isotopic composition of common lead. This is commonly estimated from some model of the isotopic evolution of average crustal lead (Cumming and Richards, 1975; Stacey and Kramers, 1975). When using the two-stage model of Stacey and Kramers (1975), common lead has $^{206}Pb/^{204}Pb \leq 18.700$ and $^{207}Pb/^{204}Pb \leq 15.628$, and its isotopic composition is a function of age constrained by a growth curve with time-integrated $^{238}U/^{204}Pb$ ratio (commonly denoted μ_2) of 9.735 since 3.7 Ga, the younger part of which is shown in a $^{207}Pb/^{204}Pb$ vs. $^{206}Pb/^{204}Pb$ isochron diagram in Fig. 5a. For a recent, general introduction to lead isotope systematics and the properties of this type of diagram, see Halla (2018). The use of an average crustal lead isotope model for common lead is appropriate if common lead has been incorporated at the time of crystallization of the zircon, and the magma from which it crystallized was derived from a relatively primitive crustal source. If common lead was incorporated later, e.g. during recent weathering, this type of common lead isotope composition will not be appropriate.

Lead remobilized during weathering will have a higher $^{206}Pb/^{207}Pb$ ratio than the average, unweathered whole-rock, due to selective release of radiogenic lead from uranium-enriched minerals (Harlavan and Erel, 2002). In an igneous rock, such radiogenic lead will be counteracted by release of unradiogenic lead from U-free minerals such as K-feldspar. In a quartz arenite with low contents of detrital feldspar and above-average enrichment in heavy minerals including zircon, the capacity of "buffering" the isotopic composition of lead remobilized during weathering to near-crustal-average ratios will be much lower than in a granite undergoing weathering.

The effect of selective release of radiogenic lead with elevated $^{206}Pb/^{207}Pb$ (and hence low $^{207}Pb/^{206}Pb$ ratio) can be illustrated in the Pb-Pb isochron diagram in Fig. 5a. In this diagram, the radiogenic lead component in an unaffected zircon will plot on a secondary isochron whose slope is a function of the age of the zircon (i.e. of the rock in which it crystallized), and whose initial lead composition is given by the composition of common lead at the time of crystallization, for example the 2.0 Ga composition of average crust with μ_2 = 9.735 shown in Fig. 5a. At the present time, a 2.0 Ga zircon will plot on the secondary isochron at a high $^{206}Pb/^{204}Pb$ ratio (off the scale of Fig. 5a). A mixture of such highly radiogenic lead and unradiogenic initial lead released during weathering will also plot on this line, somewhere between the two endmembers. An example of a mixture corresponding to a $^{238}U/^{204}Pb$ ratio of 21 since original crystallization (denoted μ_3) is shown in Fig. 5a. At $^{206}Pb/^{204}Pb$ = 22.80, $^{207}Pb/^{204}Pb$ = 16.13, this lead is significantly more radiogenic than both the unradiogenic lead component in any U-free mineral in the sample, and average crustal lead at any time. The change in $^{206}Pb/^{204}Pb$ is larger than the corresponding shift in $^{207}Pb/^{204}Pb$, and hence the $^{206}Pb/^{207}Pb$ ratio (1.41) will be higher than ratios used in common lead corrections using average crustal lead compositions ($^{206}Pb/^{207}Pb \leq 1.21$).

In a conventional U-Pb concordia diagram, the slope of the common lead line is defined by the $^{206}Pb/^{207}Pb$ ratio of the common lead component, which is situated at infinity in this type of diagram (Fig. 5b). In a Tera-Wasserburg concordia diagram, the composition of common lead is given by points on the $^{207}Pb/^{206}Pb$ axis; crustal lead with $^{206}Pb/^{207}Pb$ = 1.21 at a point with coordinates (0, 0.83) and the more radiogenic mixture with $^{206}Pb/^{207}Pb$ = 1.41 at the point (0, 0.71) (Fig. 5c). At minor common ^{206}Pb, the corrected composition is relatively insensitive to the composition of common lead used (Andersen, 2002). At larger corrections (exceeding ca. 1%), and with the elevated $^{206}Pb/^{207}Pb$ (and hence low $^{207}Pb/^{206}Pb$) ratios to be expected for mobile lead during surface weathering in old quartz arenites, this will be different. The slope of the mixing line between radiogenic lead and common lead in this diagram is in general such that even a considerable error in $^{206}Pb/^{204}Pb$ ratio of common lead will only cause a minor

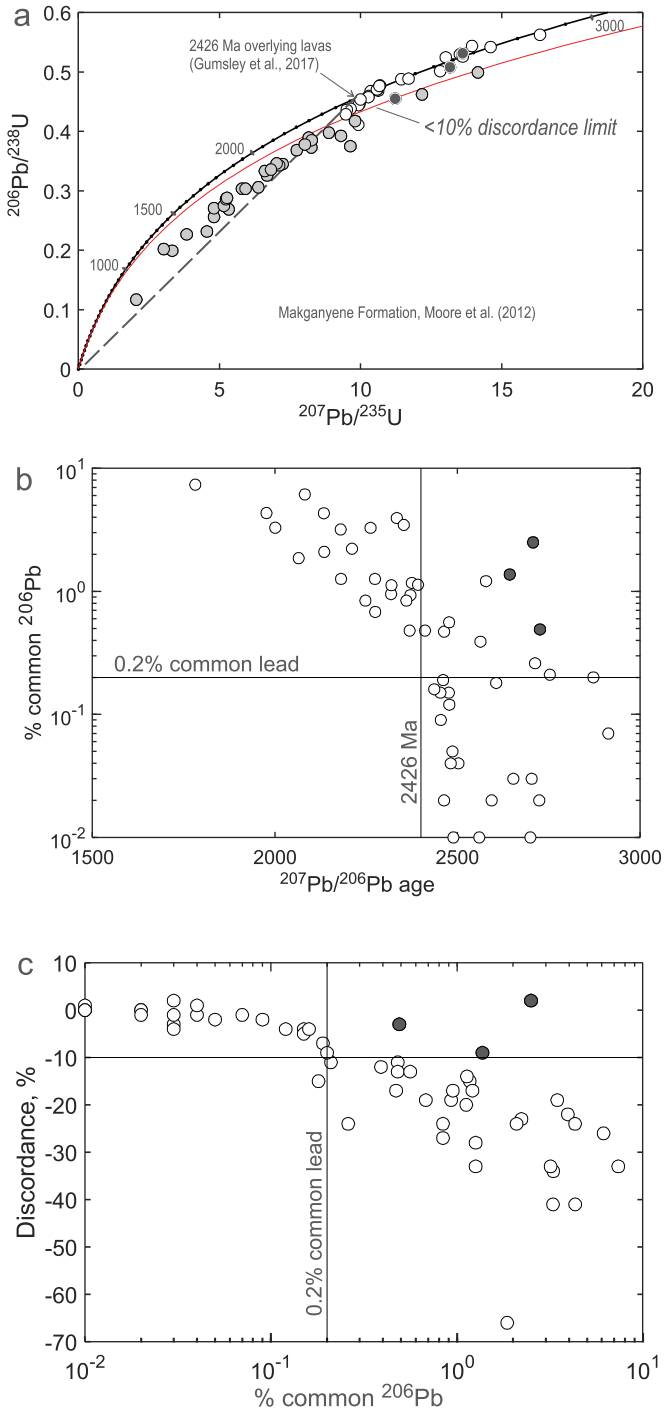

Fig. 6. Detrital zircon U-Pb data from diamictite of the Palaeoproterozoic Makganyene Formation, South Africa, used to illustrate some side effects of common lead correction of detrital zircon ages. For background information on the sample, see Table 1.

a: SIMS U-Pb data for 61 zircons from Moore et al. (2012), with the 10% discordance limit used by the original authors. Errors and error correlations have been omitted to reduce clutter in the diagram. The dotted discordia line has an upper intercept given by the U-Pb baddeleyite age of the overlying Ongeluk lavas (2426 ± 3 Ma, Gumsley et al., 2017). Grey and black points have been corrected for more than 0.2% common lead. The three corrected analyses indicated by black fill fall within the 10% discordance limit at ages > 2500 Ma. An alternative explanation for these is discussed in the text.

b: Percent common lead vs. corrected $^{207}Pb/^{206}Pb$ age. Black points as in (a).

c: Percent common lead before correction vs. discordance. The three black points (as in a and b) are heavily common lead-corrected points that pass the 10% discordance filter, but which are excluded when the $^{206}Pb/^{204}Pb$ ratio or the amount of common lead is used to filter data.

systematic error in the corrected $^{206}Pb/^{238}U$ or $^{238}U/^{206}Pb$ ratios, but the corrected $^{207}Pb/^{235}U$ ratio will be severely biased towards low values if too low a $^{206}Pb/^{207}Pb$ (i.e. too high $^{207}Pb/^{206}Pb$) ratio is used for common lead, as illustrated by the" overcorrected ^{207}Pb" point in Fig. 5b and the "overcorrected $^{207}Pb/^{206}Pb$" ratio in Fig. 5c. This effect increases with the amount of common lead removed by the correction, and as a result, zircons with high common lead contents are likely to be selectively overcorrected in ^{207}Pb, and hence yield $^{207}Pb/^{206}Pb$ ages

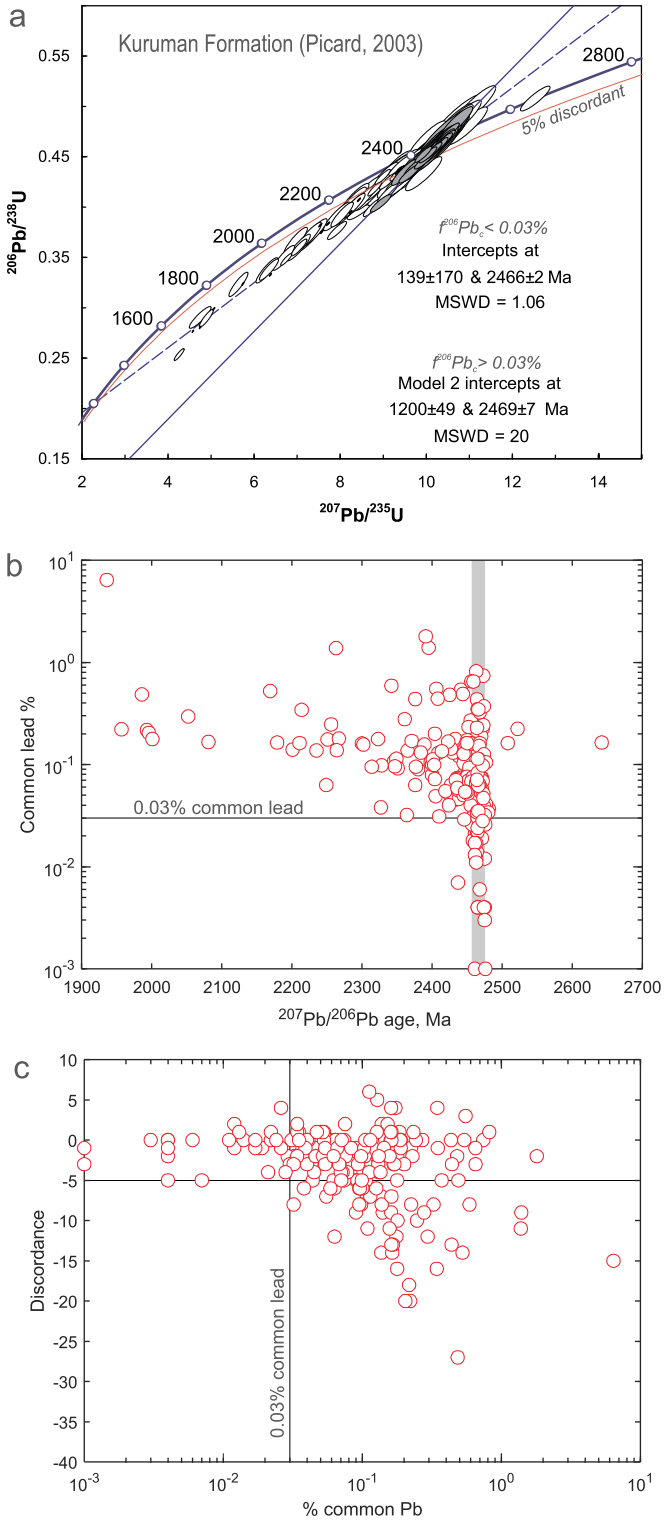

(caption on next page)

Fig. 7. U-Pb data from detrital zircon the Palaeoproterozoic Kuruman Formation, South Africa used to illustrate some side effects of common lead correction of detrital zircon ages. For background information on the samples, see Table 1.
a: Ion microprobe U-Pb data for 223 detrital zircons analysed by SIMS (Pickard, 2003). Grains shown with shaded error ellipses have common lead < 0.03%, and define a lead-loss line with an upper intercept of 2466 ± 2 Ma and a lower intercept within error of zero. The remaining grains (white fill) are common-lead corrected; the upper intercept is indistinguishable from the other within error, but the lower intercept has increased to 1200 Ma (dashed line). $f^{206}Pb$ is the percentage of common ^{206}Pb that has been removed by the 204-correction.
b: Percent common lead vs. corrected $^{207}Pb/^{206}Pb$ age.
c: Percent common lead before correction vs. discordance.

that are too young. The composition of the mixture of unradiogenic lead and unsupported radiogenic lead is likely to be variable, and impossible to estimate with confidence (e.g. Grauert et al., 1974).

3.3. Examples: the Makganyene and Kuruman formations, South Africa

SIMS U-Pb data on detrital zircon from diamictite of the Palaeoproterozoic Makganyene Formation (Fig. 6, data from Moore et al., 2012) and mudstones of Kuruman Formation (Fig. 7, data from Pickard, 2003) in the Griqualand West Basin, South Africa, illustrate some unintended effects of common lead correction on detrital zircon U-Pb data.

The Makganyene Formation was deposited prior to the lavas of the overlying 2426 ± 3 Ma Ongeluk Formation (Gumsley et al., 2017). By applying a 10% discordance filter to their data, Moore et al. (2012) obtained acceptable detrital zircon ages in the range 2436–3666 Ma for 30 of 61 data points, thought to reflect the ages of protosource rocks. The 31 data points rejected by the discordance filter show a pronounced tendency towards much younger $^{207}Pb/^{206}Pb$ ages, i.e. they are discordant grains plotting above a lead-loss line from 2426 Ma to zero in Fig. 6a. It should be noted that the amount of common lead removed is correlated with decreasing $^{207}Pb/^{206}Pb$ age and increasing discordance (Fig. 6b,c).

The banded iron formation succession of the Kuruman Formation (Fig. 7) occurs at a lower stratigraphic level in the Griqualand West Basin than the Makganyene Formation. SIMS data on detrital zircon separated from mudstones in the succession indicate a main age fraction at ca. 2460 Ma, suggesting a dominant provenance component from volcanic sources coeval with BIF sedimentation (Pickard, 2003), and minor older components. Common lead contents range from zero to 6.4% common ^{206}Pb, and raw data have been corrected by a conventional ^{204}Pb correction (Pickard, 2003). Linear regression of 48 grains with common-^{206}Pb < 0.03% (assuming error correlation of 0.9) yields a discordia line from an upper intercept at 2466 ± 2 Ma, to a 139 ± 170 Ma lower intercept, i.e. within error of zero (filled signature in Fig. 7a). Grains that have been corrected for more than 0.03% common lead show divergent behaviour (Fig. 7b, c). One group of grains retains $^{207}Pb/^{206}Pb$ ages close to 2460 Ma after correction, suggesting that common lead in these analyses originate from the mounting medium or the sample surface, as suggested by Williams (1998). Another group of grains with common lead above 0.03% show a correlation between common lead content, low $^{206}Pb/^{207}Pb$ age after correction and discordance similar to that observed in the Makganyene diamictite (Fig. 7b, c). Regression of 174 grains corrected for more than 0.03% common lead gives a poorly defined line (MSWD = 20) with an indistinguishable model-2 upper intercept at 2469 ± 7 Ma, but with a lower intercept at 1200 ± 49 Ma.

The conventional interpretation of such discordant U-Pb data is that the zircons have suffered ancient, post-depositional lead loss, perhaps combined with additional loss of radiogenic lead in recent time. However, this cannot account for the correlations between low $^{207}Pb/^{206}Pb$ age, the percentage of normal discordance and the amount of common lead removed by correction (Figs. 6 and 7). Continuous, diffusion-driven lead loss (Tilton, 1960) would be able to produce discordant grains with anomalously young $^{207}Pb/^{206}Pb$ ages and discordia lines with meaningless lower intercepts, but will also not be able to create the correlation between discordance and common lead content observed.

Near-surface rocks in southern Africa have been exposed to deep weathering since the late Cretaceous (Partridge et al., 2006). Chemical weathering under warm climatic conditions will affect zircon, especially radiation damaged parts of crystals (e.g. Balan et al., 2001), causing both loss of radiogenic lead and uptake of mobile lead (e.g. Stern et al., 1966; Black, 1987; Pidgeon et al., 2013). In a sedimentary rock undergoing weathering, such mobile lead would be more radiogenic than average crust (Fig. 5a), and the use of any crustal average common lead composition for correction will lead to overcorrection of the $^{207}Pb/^{235}U$ ratio, which can account for the anomalously young $^{207}Pb/^{206}Pb$ ages and meaningless lower intercepts in Figs. 6 and 7.

4. Age bias and Hf isotope systematics

The Lu-Hf isotope system of zircon is much more robust than the U-Pb system. Thus, a process that modifies the Pb/U ratio of a zircon will commonly leave its Lu/Hf and $^{176}Hf/^{177}Hf$ ratios unaffected. Due to the low $^{176}Lu/^{177}Hf$ of zircon (commonly of the order of 0.001, which, for example, is the average of the zircons in samples MEMG3 and MEMG4 reported in Supplementary Table S1), the change of $^{176}Hf/^{177}Hf$ due to in-situ decay of ^{176}Lu will be slower than that of whole-rocks. In this paper, we express time-corrected $^{176}Hf/^{177}Hf$ ratios of zircons in terms of the epsilon-Hf parameter, describing the deviation from the evolution curve of CHUR (Chondritic Uniform Reservoir) at the time of crystallization (Dickin, 2005). An observed, present-day $^{176}Hf/^{177}Hf$ ratio of a zircon can be back-calculated to an epsilon-Hf value at the $^{207}Pb/^{206}Pb$ age of the zircon by extrapolating along a straight growth line in an epsilon-Hf vs. time diagram whose slope is a function of the $^{176}Lu/^{177}Hf$ ratio of the zircon. In a diagram of $^{176}Hf/^{177}Hf$ versus time, the slope would be close to zero, because of the very low $^{176}Lu/^{177}Hf$ ratio of zircon. However, in an epsilon-Hf versus time diagram, the line has a pronounced positive slope, as a result of the much higher $^{176}Lu/^{177}Hf$ value (0.0336) for CHUR, which, by definition, has a slope of zero in this type of diagram. If no lead loss has taken place after initial crystallization of the zircon, or if lead loss is recent, the $^{207}Pb/^{206}Pb$ age of the zircon reflects its primary crystallization age, and the calculated epsilon-Hf will represent that of the protosource rock at the time of its crystallization. If, on the other hand, the zircon has lost lead significantly before the present time, epsilon-Hf at the observed, apparent $^{207}Pb/^{206}Pb$ age no longer represents the properties of the protosource. As far as ancient lead loss results from a single and well-constrained event (thermal, diagenetic, weathering), zircons having suffered variable degrees of lead loss will plot along a linear trend in an epsilon-Hf vs. time diagram which starts at the primary age and Hf isotopic composition of the protosource and terminates at the age of the thermal event (Amelin et al., 2000). In some cases, Hf isotope data may therefore help to distinguish between zircon fractions affected by lead loss and those that originate from distinct protosources.

How this can be done is illustrated by combined U-Pb and Lu-Hf data for detrital zircon in a sample of sandstone from the Palaeoproterozoic Waterberg Group, South Africa (SA16–402, Table 1) shown in Fig. 8a, b (data from Andersen et al., 2019). Zircons in this sample comprise a major age fraction between 2000 and 2150 Ma, and a range of early Palaeoproterozoic and Neoarchaean (2200–2800 Ma) zircons. The age of deposition of this sandstone cannot be older than the age of the Bushveld complex at 2055 Ma (Zeh et al., 2015) or younger than ca. 1870 Ma cross-cutting mafic intrusions (Hanson et al., 2004). The 2000–2150 Ma age fraction in this sample is in principle open to two interpretations: It can represent one or more protosources that formed in this age range, or it may be caused by extensive lead loss

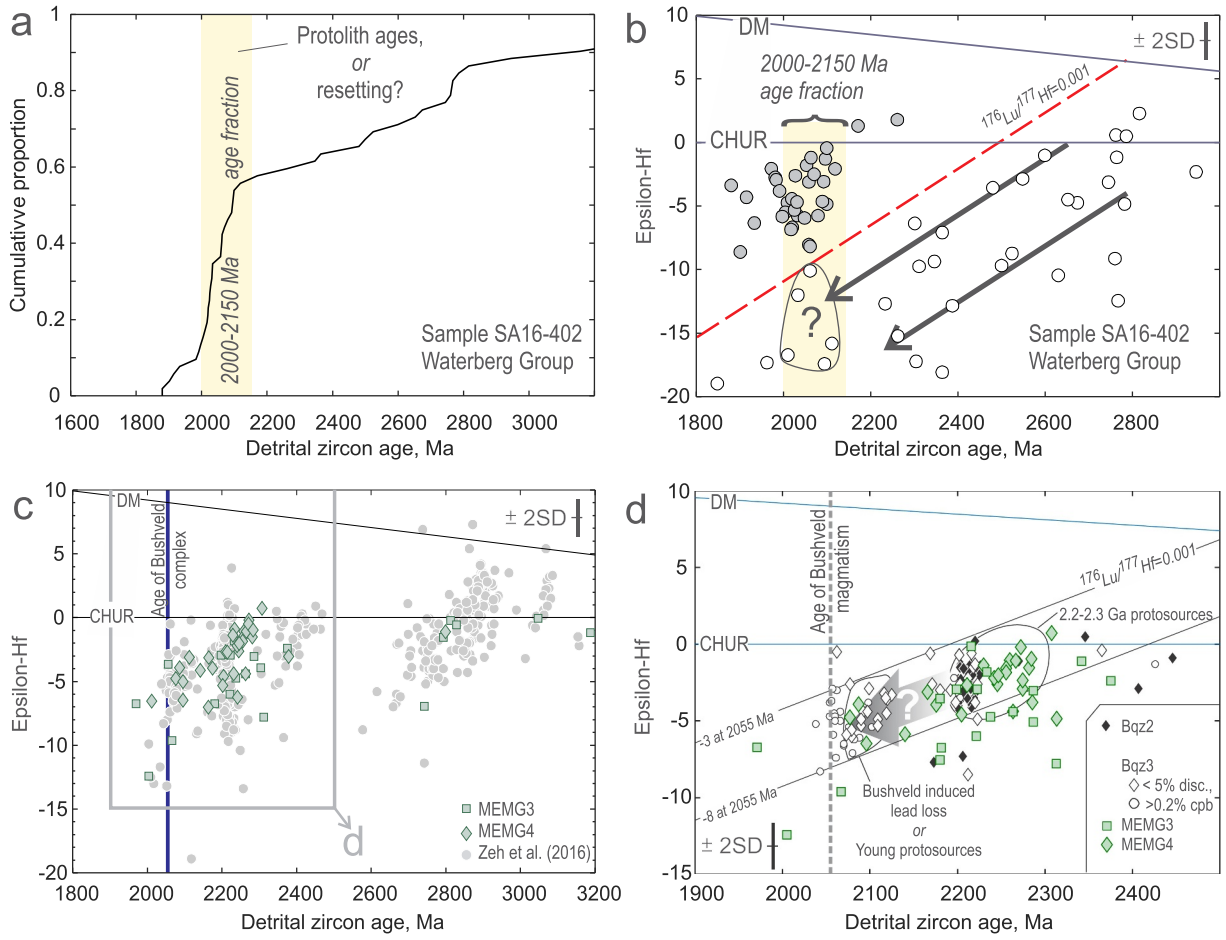

Fig. 8. a: Cumulative distribution of $^{207}Pb/^{206}Pb$ ages for detrital zircons in a sample of the Palaeoproterozoic Waterberg Group, South Africa (Andersen et al., 2019, see Table 1 for further information). Note the prominent age fraction in the 2000 Ma to 2150 Ma range. For background information on the sample, see Table 1.
b: LA-MC-ICPMS epsilon-Hf vs. $^{207}Pb/^{206}Pb$ age for detrital zircons in the sample shown in (a) (data from Andersen et al., 2019). The zircons shown in grey cannot have originated from any of their older, white counterparts by concealed lead loss, since the trajectory of a zircon losing lead is controlled by the $^{176}Lu/^{177}Hf$ ratio of the zircon (in this example set to 0.001), and lead loss, for example at the time of emplacement of the Bushveld complex at 2055 Ma cannot cause older zircons to cross the dashed line through epsilon-Hf at 2500 Ma. However, zircons in the 2000–2150 Ma age range with epsilon-Hf < -10 (highlighted by question mark) may have been affected by concealed lead loss.
c: Epsilon-Hf in detrital zircon from samples MEMG3 and MEMG4 (data from Supplementary Table S1) compared to the total dataset of Zeh et al. (2016), comprising 657 grains analysed for Lu-Hf (Table 1).
d: Detail of the epsilon-Hf vs. time diagram for the Magaliesberg Formation, showing samples MEMG3 and MEMG4 from the present study, and BQz2 and BQz3 from Zeh et al. (2016). For sample BQz3, zircons that are concordant within ± 5% that are common lead-free, and those that have been corrected for more than 0.2% common ^{206}Pb are shown with different signatures. The lines through epsilon-Hf = −3 and −8 at 2055 Ma have slopes corresponding to $^{176}Lu/^{177}Hf = 0.001$. The 2080–2150 Ma zircons in this sample may have been derived from a separate protolith, or they may be equivalents of zircon of the older age fraction (2200–2300 Ma) plotting between these limits that have lost radiogenic lead at 2055 Ma, as indicated by the shaded arrow with question mark.

affecting early Palaeoproterozoic and Neoarchaean zircons, for example resulting from contact metamorphism of a sedimentary precursor by the emplacement of Bushveld magmas at 2055 Ma. In this example, Hf isotope data give helpful information (Fig. 8b). A straight line through epsilon-Hf = 0 at 2500 Ma with a slope corresponding to an average zircon $^{176}Lu/^{177}Hf$ ratio of 0.001 provides a convenient reference line in the diagram that cannot be crossed by older zircons whose $^{207}Pb/^{206}Pb$ ages are changed by subsequent loss of radiogenic lead. Most of the 2000–2150 Ma zircons in this sample have epsilon-Hf higher than −10 (grey points in Fig. 8b), plotting above this line. In contrast, zircons older than ca. 2200 Ma, and a minor fraction of the 2000–2150 Ma zircons plot below the line (white points in Fig. 8a). Since lead loss at 2055 Ma or later would cause zircons in this group to shift to younger ages along straight lines parallel to the reference line, lead loss from zircons in the older fraction cannot account for any of the high epsilon-Hf zircons in the 2000–2150 age range, which make up a majority of this age fraction. The 2000–2150 Ma zircons with epsilon-Hf > −10 must therefore originate from one or more protosources with younger age and different crustal Lu-Hf evolution history than the source(s) of the older zircons in this sample. However, a minor fraction of 2000–2150 Ma zircons with low epsilon-Hf (< −10, indicated by question mark in Fig. 8b) can either be older grains that have suffered concealed lead loss, or grains derived from 2000 to 2150 Ma protosources whose Lu-Hf characteristics must have been different from that of the zircons with similar age but higher epsilon-Hf. In this example, Hf isotope data can help to define one sub-fraction of zircons that has a robust protosource signature and that cannot have been generated by concealed lead loss from older age fractions, and to point out zircons whose origin is less certain, and which must therefore be interpreted with care.

Unfortunately, Hf isotope data cannot always be used to distinguish between mutually exclusive interpretations of U-Pb age fractions. Data on Palaeoproterozoic detrital zircon in the Magaliesberg Formation, whose U-Pb distributions were shown in Fig. 2b and discussed in

Section 2.2 provide an example. The 2080–2130 Ma age fraction in sample BQz3 was interpreted by Zeh et al. (2016) as reflecting protosource ages. The alternative interpretation is that this age fraction consists of 2200–2300 Ma or older zircons that have suffered concealed, partial lead loss at the time of emplacement of the Bushveld complex at 2055 Ma. Lu-Hf isotope data were published by Zeh et al. (2016), and data for samples MEMG3 and MEMG4 are presented in this study (Supplementary Table S1). There is general overlap between the Palaeoproterozoic zircons in all these samples, with clusters at epsilon-Hf = −10 to 0 at 2200–2300 Ma and −8 to −3 at 2050–2150 Ma (Fig. 8c). Epsilon-Hf values of the zircons in sample BQz3 of Zeh et al. (2016), which has a major age fraction at 2080–2130 Ma, are moderately negative. All but one of the grains in this sample that are younger than 2200 Ma plot between straight lines with slope corresponding to $^{176}Lu/^{177}Hf = 0.001$ drawn through points at 2055 Ma with epsilon-Hf = −3 and −8, respectively (Fig. 8d). A majority of zircons in the 2200–2300 Ma age range in samples BQz2, MEMG3 and MEMG4 also fall between these two lines (Fig. 8d). Loss of radiogenic lead from zircons in this, older group will shift the grains along straight lines between the two, limiting lines, as indicated by the grey arrow in Fig. 8d. Zircons that have lost a considerable part of their radiogenic lead at 2055 Ma will be shifted to overlap with the younger age fraction in BQz3. Hf isotope data will therefore not be able to distinguish between older grains that have suffered concealed lead loss, and grains that have been derived from 2080 to 2150 Ma protosources with a similar Hf isotope signature.

5. Discussion

The features reviewed in this paper are well-known aspects of the U-Pb and Lu-Hf systematics of zircon, and most published detrital zircon geochronology studies take at least some of the effects illustrated here into consideration. However, the examples presented above suggest that some bias is likely to remain hidden within what is commonly regarded as acceptable data. Some of the consequences for geological interpretation of detrital zircon data are discussed in the following paragraphs.

5.1. Spurious age fractions

The potentially most damaging violation of the assumption of qualitative representativity of detrital zircon age data to appear from the present review is the potential of ancient lead loss processes to generate spurious age fractions that have no counterpart in the protosources. Even as strong a discordance limit as ± 5% may fail to identify grains that have suffered post-depositional lead loss causing shifts in the $^{207}Pb/^{206}Pb$ ages of several hundred million years (Figs. 1 and 2d). Unfortunately, Hf isotope data cannot always be used to distinguish between zircon from genuinely young protosources and older zircons that have lost lead after deposition, as was illustrated by the data from the Magaliesberg Formation (Section 4 and Fig. 8d).

Ancient lead loss in a suite of detrital zircons may be due to the thermal effect of younger magmatic intrusions. In Mesoproterozoic sandstone of the Eriksfjord Formation in southern Greenland, a large proportion of detrital zircons of variable primary age, origin and Hf isotope composition were shifted to a formally concordant but anomalously young age by the thermal effects of magmatism on the host sediment a relatively short time after its deposition (Andersen, 2013). Despite the significant amounts of radiogenic lead lost in this process, most zircons retained a magmatic, oscillatory zoning pattern in cathodoluminescence images, with only subtle indications of overprint (see Andersen, 2013 for illustration). The resulting, spurious age fraction could be recognized as such from an unreasonably large range in Hf isotopic composition of 38 epsilon units at the time of the resetting event. Intrusion of the Bushveld magmas into the quartz arenites of the Magaliesberg Formation at 2055 Ma would in principle have induced a far larger thermal effect than that experienced by the Eriksfjord sandstone, with the possibility of a shift in detrital zircon ages towards the age of contact metamorphism, while keeping within the ± 5% discordance envelope (Fig. 2d).

A 2200–2300 Ma age fraction is prominent in all of the samples so far analysed from the Magaliesberg Formation (Schröder et al., 2016; Zeh et al., 2016, this study). Similar age fractions are found in other Palaeoproterozoic deposits in southern Africa, e.g. in the Elim group of the Griqualand West Basin, South Africa (van Niekerk, 2006; Dreyer, 2014) and in the Segwagwa Group of Botswana (Mapeo et al., 2006). The source of these zircons remains controversial, but observations of 2200–2300 Ma, zircon-bearing tuff layers in sedimentary rocks of the Transvaal Supergroup (Rasmussen et al., 2013) indicate that there was volcanic activity of relevant composition somewhere along the margin of the Kaapvaal Craton in this time period. There is thus no reason to doubt the genuine protosource significance of this age group of zircons, although the source itself remains to be identified.

The interpretation of the 2080–2130 Ma age fraction as representing protosource ages was questioned by Beukes et al. (2019). The observation to be made from Figs. 2 and 8d in this study is that the interpretation of the 2080–2130 Ma age fraction as representing protosource ages may be less robust than suggested by Zeh et al. (2016), because complete overlap in epsilon-Hf of potential, young protosurce (s) and a spurious age fraction generated by concealed lead loss during or after emplacement of the Bushveld complex.

Spurious age fractions in the Eriksfjord sandstone and potentially in the Magaliesberg quartzite are due to thermally induced lead loss related to known magmatic intrusions. Ancient lead loss due to weathering processes will have similar effects, and is equally likely to remain undetected by conventional discordance filters. This suggests that detrital zircon data from palaeosols, or other fossil weathering zones should be treated with great care. Although trace element-based methods for identifying more reliable analyses have been proposed (e.g. Bell et al., 2016), these are not part of the routine analytical set-up. Additionally, these trace element analyses are often not performed on exactly the same spot as the U-Pb analysis, and their interpretation may therefore become ambiguous.

Apparently concordant, spurious age fractions may also appear as an unintended effect of common lead correction. When common lead correction is applied to zircons that have lost a minor amount of lead in recent weathering processes, overcorrection of the $^{207}Pb/^{235}U$ ratio may result in formally concordant grains whose $^{207}Pb/^{206}Pb$ ages are systematically younger than their true crystallization age. It may be speculated that such effects have produced apparently concordant zircons at ca. 2200 Ma in the Makganyene Formation diamictite reported by Beukes et al. (2013) and Ngobeli et al. (2018), but the underlying data have not yet been published in a way that allows a critical review.

5.2. The “youngest detrital zircon age (fraction)” and “maximum depositional age”

There is in principle no necessary relationship between ages of zircon-forming processes in a protosource terrane and the age of the sediment in which detrital zircons are finally deposited. For example, a sample of beach sediment from a locality near Durban, South Africa, gave a minimum detrital zircon age of 241 Ma (Andersen et al., 2016a), significantly overestimating the Recent age of deposition of this sand. The use of the “youngest detrital zircon age” or age fraction to define a maximum age of deposition for a clastic sediment is thus problematic even when the age data are unbiased by effects discussed in this paper, but is nevertheless in common use. The general lead-loss scenario illustrated in Fig. 1 raises some fundamental questions that must be answered before data can be used to define limits for the age of sedimentation: The age of the concordant *a* zircon (t_1) would in general be recognized as an undisputed primary crystallization age (i.e. a protosource age), especially if supported by a cathodoluminescence or

electron-backscatter image showing undisturbed, magmatic zonation features (e.g. Corfu et al., 2003), and t_1 is then a valid upper limit for the deposition age of its host sediment. Zircon *b* plots within the permissible discordance envelope, and its $^{207}Pb/^{206}Pb$ age (t_3) could be invoked as a younger maximum limit for the sedimentation age, some 275 Ma younger than t_1. However, if the minor discordance of *b* is due to lead loss at t_2 or t_4 rather than recent lead loss, t_3 is a meaningless age. The significance of t_2 and t_4 is open to interpretation. If the lead loss events indicated by these lower intercept ages took place prior to final deposition of the zircon and its host sediment, it is t_2 or t_3 that defines the maximum depositional age, some 600–850 Ma younger than t_1. If, on the other hand, these lower intercept ages reflect lead-loss processes after deposition of the host sediment, t_2, t_3 and t_4 have no significance for the age of deposition. Furthermore, the potential of common lead corrections to generate formally concordant, spurious age fractions that appear younger than their true age add further complexity to the interpretation of the youngest detrital zircon ages.

Conflicts between maximum limits for depositional age inferred from detrital zircon data and "hard" evidence from other sources (e.g. robust ages for crosscutting dykes or overlying volcanic rocks) will almost always be due to unrecognized problems in the detrital zircon data that have caused bias towards too young ages of the critical age fraction, calling for utmost caution when interpreting such data.

5.3. Can discordant zircon give useful information?

Reimink et al. (2016) published a method to extract potentially meaningful upper and lower intercept ages from U-Pb data on suites of discordant detrital zircons. A probability density surface is constructed over the $^{207}Pb/^{235}U$-$^{206}Pb/^{238}U$ plane, taking error correlation and relative degree of discordance into account. This can be transformed into likelihood estimates for combinations of upper and lower intercept ages by summing probability densities along cords between pre-defined upper and lower intercept ages. The outcome is a 2D map of likelihood for upper and lower intercept ages, and marginal likelihood profiles for upper and lower intercept ages, respectively. Maxima represent the best estimates of primary crystallization ages and ages of disturbance for significant fractions of discordant detrital zircons in the sample. The mathematics of the method is explained in some detail in the original paper by Reimink et al. (2016). This method has been applied to discordant data from the Makganyene and Magaliesberg formations (Fig. 9).

The maximum likelihood peak of upper intercept ages for the Makganyene Formation overlaps the interquartile range of concordant zircon in the sample (Moore et al., 2012), but there is a significant, non-zero likelihood of finding upper intercepts both significantly older than any concordant zircon age observed in the sample, and ages younger than any estimate of the depositional age of this diamictite (Fig. 9a). This is coupled with maxima for lower intercepts in the Neoproterozoic and at ca. 250 Ma.

The three different datasets from the Magaliesberg Formation show even less clear behaviour. The data from Zeh et al. (2016) show a very broad likelihood maximum for upper intercepts in the late Archaean, and an equally poorly defined lower intercept maximum in the Phanerozoic (Fig. 9b). In contrast, the smaller dataset of Schröder et al. (2016) defines as sharp likelihood maximum for the upper intercept that overlaps with the narrow interquartile range of concordant $^{207}Pb/^{206}Pb$ ages, and a lower intercept peak at ca. 125 Ma (Fig. 7c). Unfortunately, the upper intercept likelihood remains high, and increasing to ages > 4500 Ma, which cannot have any geological significance. The data for samples MEMG3 and MEMG4 from this work (Fig. 9d) show maximum likelihood peaks for upper intercepts overlapping reasonably well with the early Palaeoproterozoic and Archaean age fractions observed in the concordant part of the dataset, but again suggesting that elevated likelihood for upper intercepts extends into the early Archaean. The lower intercepts define a broad likelihood peak

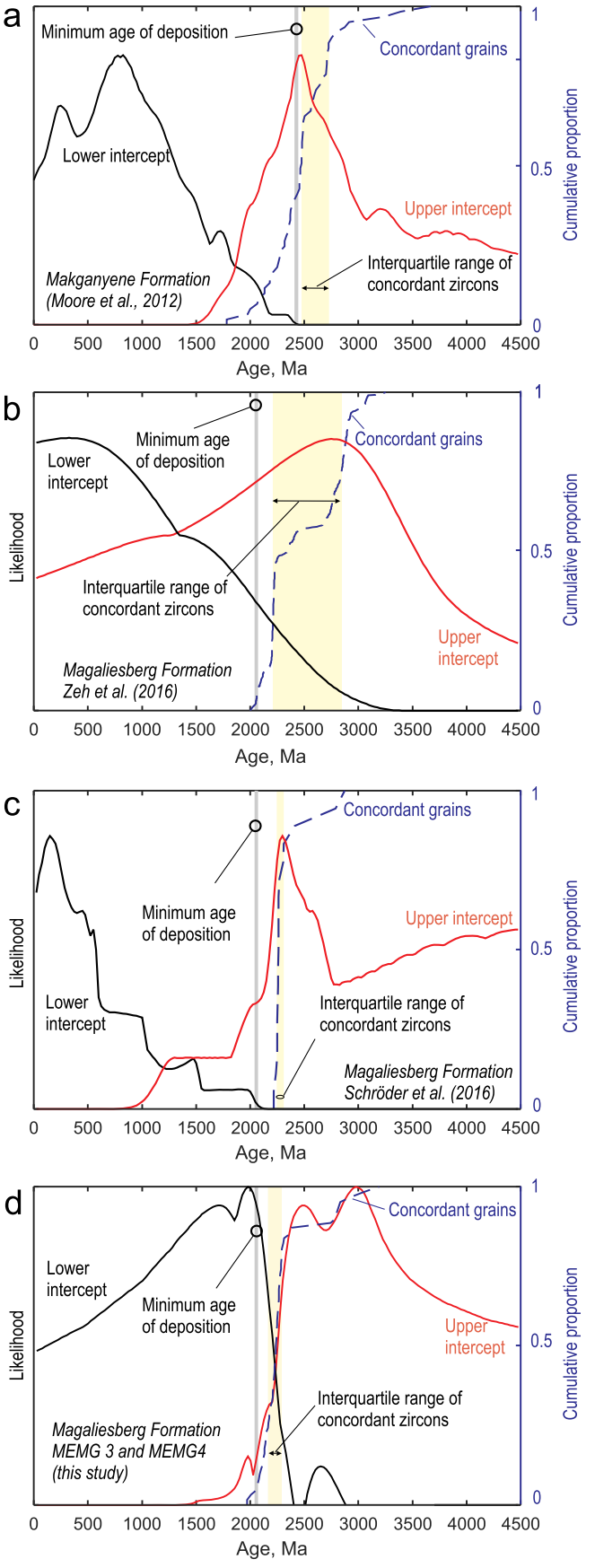

(caption on next page)

Fig. 9. Likelihood estimates for upper and lower intercept age for discordant zircon in Makganyene and Magaliesberg formations (data from Moore et al., 2012; Schröder et al., 2016 and Table 1) by the algorithm of Reimink et al. (2016), compared to cumulative distribution curves for concordant grains in the same datasets (dashed lines referring to right hand scale). Also shown are minimum limits for the age of deposition defined by overlying volcanic rocks (a, data from Gumsley et al., 2017) and the emplacement age of the Bushveld complex (b, c, d, data from Zeh et al., 2015), and interquartile age ranges for the concordant detrital zircon grains.

with a maximum in the late Palaeoproterozoic, which is superposed by a sharp maximum overlapping with the age of the Bushveld complex.

The examples above show that the method of Reimink et al. (2016) may give upper intercept estimates that may be geologically meaningful (Fig. 9c, d), but also results that are difficult to interpret, or are geologically meaningless (upper intercept peaks in Fig. 9a, b, elevated early Archaean likelihoods in Fig. 9c, d). The lower intercept maxima indicated in Fig. 9 are all significantly younger than the respective depositional ages, and may possibly be related to post-depositional lead loss events. However, it is difficult to relate these peaks to known geological events, the reason may be that the method is not able to cope with data from grains that have lost lead in more than one episode (e.g. at 2055 and 0 Ma in the Magaliesberg example). It should also be noted that discordant zircons whose $^{207}Pb/^{206}Pb$ ratios have been biased by overcorrection for common lead will not automatically be recognized as such, leading to spurious results. These examples suggest that the method of Reimink et al. (2016) may give unpredictable results, and that it should be used only with great care and a good understanding of the geological history of the host sediment.

An alternative approach to moderately (≤10%) discordant zircons was proposed by Shaanan et al. (2019), making use of partial age distributions of ancient zircons as "fingerprints" of old crustal sources. Whereas this method may also give interesting information, as in the examples discussed by Shaanan et al. (2019), it is unlikely to be generally applicable (see, for example, a general discussion of similarity between old crustal domains by Andersen, 2014). Furthermore, the method is likely to encounter the problem of extracting specific information (the source fingerprint) from data that are essentially random, i.e. detrital zircons that have suffered partial concealed lead loss in the past, see Section 2.1, above.

5.4. A practical alternative to the constant discordance filter?

The examination of the U-Pb data from the Magaliesberg Formation (Fig. 2) suggests that although a constant discordance filter is likely to identify and remove points whose discordance is due to young or recent lead loss, it is also likely to let grains that have suffered even significant amounts of ancient lead loss pass undetected. The $^{207}Pb/^{206}Pb$ ratio of a zircon grain that has lost lead only in recent time, and which has not incorporated unsupported, radiogenic lead in the process, truly reflects the age of the protosource, and thus gives valid information both for construction of age distribution patterns and for recalculation of Lu-Hf isotope data. Identifying grains that have lost lead only in recent time is a non-trivial problem that probably cannot be solved from U-Pb systematics alone. However, a positive correlation between the proportion of common lead and the degree of normal discordance (Figs. 6 and 7) is an indication, although no proof, that recent weathering is an important cause of both discordance and the presence of unsupported lead, and that age bias among the discordant zircon is more likely induced by the correction for common lead than the lead loss process itself. In such a situation, it may be permissible to relax the discordance filter, and instead define a rejection limit based on the amount of common lead that has been removed by correction, or on the observed $^{206}Pb/^{204}Pb$ ratio prior to correction, as was suggested by Andersen et al. (2019).

The example from the Makganyene Formation (Fig. 6) suggests that

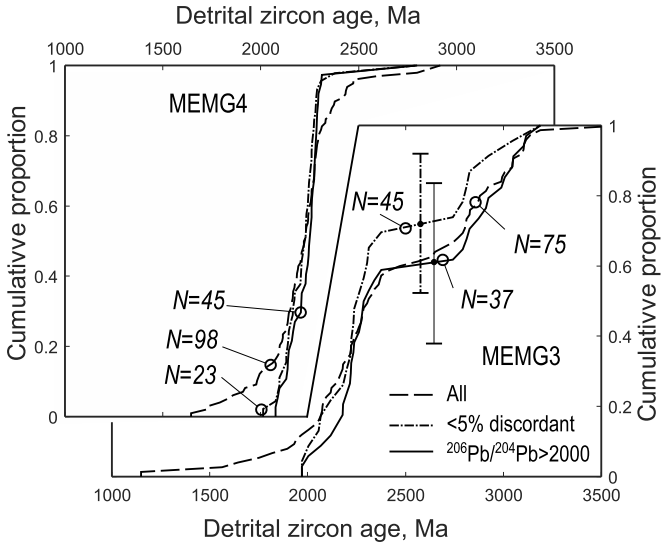

Fig. 10. The effects of two different data filtering protocols on detrital zircon distributions of samples MEMG3 and MEMG4 (Table 1, Supplementary Table S1). Numbers of grains that are retained in each of the filtered datasets are shown in the figure. Vertical bars on the filtered distribution curves of MEMG3 indicate the width of the respective confidence bands (Andersen et al., 2018b).

significant deviation from the acceptable $^{207}Pb/^{206}Pb$ age limits only occurs in grains that have been corrected for ca. 0.2% common ^{206}Pb or more. Rejecting grains with more than 0.2% common lead regardless of discordance removes the same grains as does the 10% discordance filter applied by Moore et al. (2012), but it also removes three Archaean grains which have been corrected for between 0.5 and 2.5% common lead (Fig. 6b, c), whose real ages remain unknown.

The effect of the different rejection criteria on detrital zircon age distributions can be illustrated further by samples MEMG3 and MEMG4 (Fig. 10). Both filters remove the younger age "tails". For MEMG4, the corrected distribution patterns are identical, but more grains are retained in the common-lead filtered data (45 vs. 23 grains). The response in MEMG3 is somewhat different. The Palaeoproterozoic parts of the age distributions are indistinguishable, but the fraction of Archaean zircon is higher in the common-lead filtered data. Although this difference is within the uncertainty expected from random sampling (Fig. 10), it suggests that the discordance filter has removed Archaean grains that have suffered recent lead loss, and whose ages are therefore significant.

It is probably not possible to make a general recommendation of one of the two possible rejection protocols over the other. The relative performance of the two will depend both on the age of the rock and on the post-depositional history of the sample. The detrital zircon data reviewed in this paper suggest that a rejection limit based on the $^{206}Pb/^{204}Pb$ ratio or the common lead percentage removes artifacts more efficiently than the traditional discordance limit, but this may reflect the deep, hot-climate weathering processes experienced by the rocks, and the long residence time of the zircons in the host sediment. These zircons have both suffered considerable radiation damage, and have been heavily exposed to near-surface fluids under conditions that favour reaction. The situation may be different in rocks that have been weathered in a cooler climate, or rocks that have had their weathering zones stripped off by, for example, Quaternary glaciation. In this respect, it is interesting to observe that detrital zircons in Precambrian sedimentary rocks affected by northern hemisphere glaciation (e.g. the Mesoproterozoic sandstones of the Eriksfjord Formation in Greenland; Andersen, 2013) tend to show less discordance than detrital zircon suites considered in this review.

5.5. The effect on detrital zircons in Neoproterozoic and younger deposits

The high proportion of highly discordant zircon grains encountered in the in this review appears to be a characteristic feature of Palaeoproterozoic and Archaean zircons in southern Africa, particularly those having been sampled from surface exposures (Elburg et al., 2018). These zircons have had long residence time in an undisturbed sedimentary host rock, which has been affected by deep weathering in relatively recent time. Detrital zircon in Neoproterozoic, Phanerozoic and Cenozoic deposits in the region (e.g. Andersen et al., 2016a, 2016b, 2018a; Kristoffersen et al., 2016) show lesser proportions of severely discordant and common-lead infested grains. These deposits contain a significant proportion of recycled, older sedimentary rocks, and highly metamict grains are likely to have been selectively removed during the recycling process (e.g. Markwitz and Kirkland, 2018). The degree of metamictization of a zircon depends on the U (and Th) concentration and the age of the grain (e.g. Nasdala et al., 2004). Neoproterozoic and early Phanerozoic grains have had less time to accumulate radiation damage, and are thus less vulnerable to abrasion during erosion and transport than Palaeoproterozoic and Archaean detrital zircon. These effects will combine to reduce the importance of discordance and common-lead induced bias in detrital zircon in younger deposits, but they will not remove the problem. Furthermore, any old zircon that has survived one or more recycling episodes before being deposited in its final sedimentary host may also have been affected by weathering, radiogenic lead loss and common lead uptake during previous erosion - transport - deposition cycles, thereby further complicating interpretation.

6. Conclusions

Even when widely accepted discordance criteria are applied to detrital zircon U-Pb data, systematic errors caused by concealed ancient lead loss, by underestimation of error correlation, or by correction for common lead may remain in the filtered data. Such artifacts violate the assumption of qualitative representativity of detrital zircon ages, and are detrimental to applications of detrital zircon data to geological problems. Careful scrutiny of the relationships between isotopic ratios, calculated common-lead contents, ages and discordances in the U-Th-Pb system may help detecting biased data. For this to be possible, it is important that the full set of analytical data from the mass spectrometer is published, and not only the ages calculated from them. To allow a critical examination of the effects of common lead correction on the final age data, it is important that also uncorrected U-Th-Pb data are also published, including the $^{204}Pb/^{206}Pb$ (or $^{204}Pb/^{206}Pb$) ratio prior to common lead correction.

One type of application that is especially vulnerable to age bias induced by any of the mechanisms is the use of “the youngest zircon (fraction)” to define maximum limits for age of deposition. Despite of its popularity in basin evolution and correlation studies, such interpretations of detrital zircon data should be treated with utmost caution.

Hf isotopes can often provide further guidance on the feasibility of alternative interpretations, and we would recommend that U-Pb data of detrital zircon is supported by Lu-Hf analysis on the same zircons whenever the size of the grains allows this.

The best recommendation to be given is that models based on detrital zircon data should always be kept open with respect to alternative interpretations that are compatible with the limits of discordance used and statistical errors associated with the distributions.

Acknowledgements

This work has been supported by the University of Oslo and the University of Johannesburg by “Småforsk” and “DVP” grants, respectively to TA. MAE and BM thank DST-NRF CIMERA and an NRF-IFRR grant for financial support. Thanks to Henriette Ueckermann for skilful assistance in the mass spectrometer laboratory, which was funded by NRF-NEP grant #93208, to Magnus Kristoffersen for providing software used to calculate discordance models, to Johan Petter Nystuen (UiO) and Nic Beukes (UJ) for helpful discussions and to Dr. U. Shaanan and an anonymous reviewer for constructive comments.

Appendix A. Supplementary data

Supplementary data to this article can be found online at https://doi.org/10.1016/j.earscirev.2019.102899.

References

Amelin, Y., Lee, D.-C., Halliday, A.N., 2000. Early-middle Archaean crustal evolution deduced from Lu-Hf and U-Pb isotopic studies of single zircon grains. Geochim. Cosmochim. Acta 64, 4205–4225.
Andersen, T., 2002. Correction of common lead in U-Pb analyses that do not report ^{204}Pb. Chem. Geol. 192, 59–79.
Andersen, T., 2005. Detrital zircons as tracers of sedimentary provenance: limiting conditions from statistics and numerical simulation. Chem. Geol. 216, 249–270.
Andersen, T., 2013. Age, Hf isotope and trace element signatures of detrital zircons in the Mesoproterozoic Eriksfjord sandstone, southern Greenland: are detrital zircons reliable guides to sedimentary provenance and timing of deposition? Geol. Mag. 150, 426–440.
Andersen, T., 2014. The detrital zircon record: Supercontinents, parallel evolution – or coincidence ? Precambrian Res. 244, 279–287. https://doi.org/10.1016/j.precamres.2013.10.013.
Andersen, T., Elburg, M., Cawthorn-Blazeby, A., 2016a. U–Pb and Lu–Hf zircon data in young sediments reflect sedimentary recycling in eastern South Africa. J. Geol. Soc. Lond. 173, 337–351. https://doi.org/10.1144/jgs2015-006.
Andersen, T., Kristoffersen, M., Elburg, M., 2016b. How far can we trust provenance and crustal evolution information from detrital zircon? A South African case study. Gondwana Res. 34, 129–148. https://doi.org/10.1016/j.gr.2016.03.003.
Andersen, T., Elburg, M.A., van Niekerk, H.S., Ueckermann, H., 2018a. Successive sedimentary recycling regimes in southwestern Gondwana: evidence from detrital zircons in Neoproterozoic to Cambrian sedimentary rocks in southern Africa. Earth Sci. Rev. 181, 43–60.
Andersen, T., Kristoffersen, M., Elburg, M.A., 2018b. Visualizing, interpreting and comparing detrital zircon age and Hf isotope data in basin analysis – a graphical approach. Basin Res. 30 (132–147), 1–16. https://doi.org/10.1111/bre.12245.
Andersen, T., Elburg, M.A., Van Niekerk, H.S., 2019. Detrital zircon in sandstones from the Palaeoproterozoic Waterberg and Nylstroom basins, South Africa: Provenance and recycling. S. Afr. J. Geol. 122, 79–96. https://doi.org/10.25131/sajg.122.00 08.
Balan, E., Neuville, D.R., Trocellier, P., Fritsch, E., Muller, J.-.P., Calas, G., 2001. Metamictization and chemical durability of detrital zircon. Am. Mineral. 86, 1025–1033.
Batumike, J.M., Griffin, W.L., Belousova, E.A., Pearson, N.J., O'Reilly, S.Y., Shee, S.R., 2008. LAM-ICPMS U–Pb dating of kimberlitic perovskite: Eocene–Oligocene kimberlites from the Kundelungu Plateau, D.R. Congo. Earth Planet. Sci. Lett. 267, 609–619.
Bell, E.A., Boehnke, P., Harrison, T.M., 2016. Recovering the primary geochemistry of Jack Hills zircons through quantitative estimates of chemical alteration. Geochim. Cosmochim. Acta 191, 187–202.
Beranek, L.P., Pease, V., Scott, R.A., Thomsen, T.B., 2013. Detrital zircon geochronology of Ediacaran to Cambrian deep-water strata of the Franklinian basin, northern Ellesmere Island, Nunavut: implications for regional stratigraphic correlations. Can. J. Earth Sci. 50, 1007–1018.
Beukes, N.J., Frei, D., Vorster, C., 2013. Detrital zircon age constraint of the Makganyene snowball earth event (South Africa) at 2.25–2.22 Ga: the youngest of four Huronian glaciations? Geol. Soc. Am. Abstr. Programs 45 (7), 340.
Beukes, N.J., de Kock, M.O., Vorster, C., Ravhura, L.G., Frei, D., Gumsley, A.P., Harris, C., 2019. The age and country rock provenance of the Molopo Farms complex: implications for Transvaal Supergroup correlation in southern Africa. S. Afr. J. Geol. 122, 39–56. https://doi.org/10.25131/sajg.122.0003.
Black, L.P., 1987. Recent Pb loss in zircon: a natural or laboratory-induced phenomenon? Chem. Geol. Isot. Geosci. Sect. 65, 25–33.
Cawthorn, R.G., Eales, H.V., Walraven, F., Uken, R., Watkeys, M.K., 2006. The Bushveld complex. In: Johnson, M.R., Anhaeusser, C.R., Thomas, R.J. (Eds.), The Geology of South Africa. Geological Society of South Africa, Johannesburg, pp. 261–281 Council for Geosciences, Pretoria.
Corfu, F., Hanchar, J.M., Hoskin, P.W.O., Kinney, P., 2003. Atlas of zircon textures. In: Hanchar, J.M., Hoskin, P.W.O. (Eds.), Zircon, Reviews in Mineralogy and Geochemistry. 53. pp. 469–500.
Cumming, G.L., Richards, J.R., 1975. Ore lead isotope ratios in a continuously changing Earth. Earth Planet. Sci. Lett. 28, 155–171.
Delattre, S., Utsunomiya, S., Ewing, R.C., Boeglin, J.-L., Braun, J.-J., Balan, E., Calas, G., 2007. Dissolution of radiation-damaged zircon in lateritic soils. Am. Mineral. 92, 1978–1989.
Dickin, A.P., 2005. Radiogenic Isotope Geology, 2nd ed. Cambridge University Press, pp. 508.
Dorland, H.C., 2004. Provenance Ages and Timing of Sedimentation of Selected Neoarchaean and Palaeoproterozoic Successions on the Kaapvaal Craton (Unpublished PhD Thesis). Rand Afrikaans University, Johannesburg 320 pp.
Dreyer, D., 2014. Provenance an Age of Palaeoproterozoic Red Beds of the Elim Group (Griqualand West, South Africa) as Determined from Detrital Zircon Age Populations.

Unpublished MSc Thesis. University of Johannesburg 206 pp.
Eizenhöfer, P.R., Zhao, G., Sun, M., Zhang, J., Han, Y., Hou, W., 2015. Geochronological and Hf isotopic variability of detrital zircons in Paleozoic strata across the accretionary collision zone between the North China craton and Mongolian arcs and tectonic implications. Geol. Soc. Am. Bull. 127, 1422–1436. https://doi.org/10.1130/B31175.1.
Elburg, M.A., Kristoffersen, M., Andersen, T., 2018. Contrasting Quality of Detrital Zircon in Samples from the Witwatersrand Supergroup. Abstracts. 2018. Geological Society of South Africa Geocongress, Johannesburg, pp. 68.
Eriksson, R.G., Altermann, W., Hartzer, F.J., 2006. The transvaal supergroup and its precursors. In: Johnson, M.R., Anhaeusser, C.R., Thomas, R.J. (Eds.), The Geology of South Africa. Geological Society of South Africa, Johannesburg; Council for Geosciences, Pretoria, pp. 237–260.
Gale, N.H., 1979. Correlated errors in U-Pb geochronology. Geochem. J. 13, 167–172.
Ge, R., Wilde, S.A., Nemchin, A.A., Whitehouse, M.J., Bellucci, J.J., Erickson, T.M., Frew, A., Thern, E.R., 2018. A 4463 Ma apparent zircon age from the Jack Hills (Western Australia) resulting from ancient Pb mobilization. Geology 46, 303–306.
Gehrels, G.E., 2014. Detrital zircon U-Pb geochronology applied to tectonics. Annu. Rev. Earth Planet. Sci. 42, 127–149.
Grauert, B., Seitz, M.G., Soptrajanova, G., 1974. Uranium and lead gain of detrital zircon studied by isotopic analysis and fission-track mapping. Earth Planet. Sci. Lett. 21, 389–399.
Gumsley, A.P., Chamberlain, K.R., Bleeker, W., Söderlund, U., de Kock, M.O., Larsson, E.R., Bekker, A., 2017. Timing and tempo of the Great Oxidation Event. PNAS 114, 1811–1816. www.pnas.org/cgi/doi/10.1073/pnas.1608824114.
Haines, P.W., Wingate, M.T.D., Kirkland, C.L., 2013. Detrital Zircon U–Pb Ages from the Paleozoic of the Canning and Officer Basins, Western Australia: Implications for Provenance and Interbasin Connections. West Australian Basins Symposium 2013, Perth, Western Australia 18 pp.
Halla, J., 2018. Pb isotopes – a multi-function tool for assessing tectonothermal events and crust-mantle recycling at late Archaean convergent margins. Lithos 320–321, 207–221.
Hanson, R.E., Gose, W.A., Crowley, J.L., Ramezani, J., Bowring, S.A., Bullen, D.S., Hall, R.P., Pancace, J.A., Mukwakwami, J., 2004. Paleoproterozoic intraplate magmatism and basin development on the Kaapvaal Craton: age, paleomagnetism and geochemistry of ~1.93 to ~1.87 Ga post-Waterberg dolerites. S. Afr. J. Geol. 107, 233–254.
Harlavan, Y., Erel, Y., 2002. The release of Pb and REE from granitoids by the dissolution of accessory phases. Geochim. Cosmochim. Acta 66 (5), 837–848.
Kielman, R.B., Nemchin, A.A., Whitehouse, M.J., Pidgeon, R.T., Belluci, J.B., 2018. U-Pb age distribution recorded in zircons from Archean quartzites in the Mt. Alfred area, Yilgarn Craton, Western Australia. Precambrian Res. 310, 278–290.
Knudsen, T.-L., Andersen, T., Whitehouse, M.J., Vestin, J., 1997. Detrital zircon ages from southern Norway – implications for the Proterozoic evolution of the southwestern Baltic Shield. Contrib. Mineral. Petrol. 130, 47–58.
Kristoffersen, M., Andersen, T., Elburg, M.A., Watkeys, M.K., 2016. Detrital zircon in a supercontinental setting: locally derived and far-transported components in the Ordovician Natal Group, South Africa. J. Geol. Soc. Lond. 173, 203–215. https://doi.org/10.1144/jgs2015-012.
Kusiak, M.A., Whitehouse, M.J., Wilde, S.A., Nemchin, A.A., Clark, C., 2013. Mobilization of radiogenic Pb in zircon revealed by ion imaging: Implications for early Earth geochronology. Geology 41, 291–294.
Ludwig, K.R., 2012. User's manual for isoplot/excel 3.75. a geochronological toolkit for microsoft excel. Berkeley Geochronol. Cent. Spec. Publ. 5, 75.
Mapeo, R.B.M., Armstrong, R.A., Kampunzu, A.B., Modisi, M.P., Ramokate, L.V., Modie, B.N.J., 2006. A ca. 200Ma hiatus between the lower and Upper Transvaal Groups of southern Africa: SHRIMP U–Pb detrital zircon evidence from the Segwagwa Group, Botswana: implications for Palaeoproterozoic glaciations. Earth Planet. Sci. Lett. 244, 113–132.
Markwitz, V., Kirkland, C.L., 2018. Source to sink zircon grain shape: constraints on selective preservation and significance for Western Australian Proterozoic basin provenance. Geosci. Front. 9, 415–430.
Mezger, K., Krogstad, E.J., 1997. Interpretation of discordant U-Pb zircon ages: an evaluation. J. Metamorph. Geol. 15, 127–140.
Moore, J.M., Polteau, S., Armstrong, R.A., Corfu, F., Tsikos, H., 2012. The age and correlation of the Postmasburg Group, southern Africa: constraints from detrital zircon grains. J. Afr. Earth Sci. 64, 9–19.
Nasdala, L., Reiners, P.W., Garver, J.I., Kennedy, A.K., Stern, R.A., Balan, E., Wirth, R., 2004. Incomplete retention of radiation damage in zircon from Sri Lanka. Am. Mineral. 89, 219–231.
Nemchin, A.A., Cawood, P.A., 2006. Discordance of the U-Pb system in detrital zircons: implication for provenance studies of sedimentary rocks. Sediment. Geol. 182, 143–162.
Ngobeli, R., Vorster, C., Beukes, N., Frei, D., Elburg, M., 2018. Detrital Zircon Ages as Young as 2.22 Ga in the Makganyene Diamictite Versus a 2.42 Ga Baddeleyite Age of the Conformably Overlying Ongeluk Lava, Postmasburg Group, Transvaal Supergroup: Urgent Resolution Required. Geocongress 2018, Johannesurg. Geological Society of South Africa, pp. 257.
Orejana, D., Martinez, E.M., Villaseca, C., Andersen, T., 2015. Ediacaran–Cambrian paleogeography and geodynamic setting of the Central Iberian Zone: constraints from coupled U–Pb–Hf isotopes of detrital zircons. Precambrian Res. 261, 234–251.
Partridge, T.C., Botha, G.A., Haddon, J.G., 2006. Cenozoic deposits of the interior. In: Johnson, M.R., Anhaeusser, C.R., Thomas, R.J. (Eds.), The Geology of South Africa. Geological Society of South Africa, Johannesburg, pp. 585–604 Council for Geosciences, Pretoria.
Pease, V., Scott, R.A., 2009. Crustal affinities in the Arctic Uralides, northern Russia: significance of detrital zircon ages from Neoproterozoic and Palaeozoic sediments in Novaya Zemlya and Taimyr. J. Geol. Soc. Lond. 166, 517–527.
Pickard, A.L., 2003. SHRIMP U-Pb zircon ages for the Palaeoproterozoic Kuruman Iron Formation, northern Cape Province, South Africa: evidence for simultaneous BIF deposition of Kaapvaal and Pilbara cratons. Precambrian Res. 125, 275–315.
Pidgeon, R.T., Nemchin, A.A., Cliff, J., 2013. Interaction of weathering solutions with oxygen and U–Pb isotopic systems of radiation-damaged zircon from an Archean granite, Darling Range Batholith, Western Australia. Contrib. Mineral. Petrol. 166, 511–523.
Pidgeon, R.T., Nemchin, A.A., Whitehouse, M.J., 2017. The effect of weathering on U–Th–Pb and oxygen isotope systems of ancient zircons from the Jack Hills, Western Australia. Geochim. Cosmochim. Acta 197, 142–166.
Rasmussen, B., Bekker, A., Fletcher, I.R., 2013. Correlation of Paleoproterozoic glaciations based on U–Pb zircon ages for tuff beds in the Transvaal and Huronian Supergroups. Earth Planet. Sci. Lett. 382, 173–180.
Reimink, J.R., Davies, J.H.F.L., Waldron, J.W.F., Rojas, X., 2016. Dealing with discordance: a novel approach for analysing U–Pb detrital zircon datasets. J. Geol. Soc. Lond. 173, 577–585. https://doi.org/10.1144/jgs2015-114.
Rubatto, D., 2017. Zircon: the metamorphic mineral. Rev. Mineral. Geochem. 83, 261–295.
Sambridge, M.S., Compston, W., 1994. Mixture modeling of multi-component data sets with application to ion-probe zircon ages. Earth Planet. Sci. Lett. 128, 373–390.
Satkoski, A.M., Wilkinson, B.H., Hietpas, J.H., Samson, S.D., 2013. Likeness among detrital zircon populations – an approach to the comparison of age frequency data in time and space. Geol. Soc. Am. Bull. 125, 1783–1799.
Schröder, S., Beukes, N.J., Armstrong, R.A., 2016. Detrital zircon constraints on the tectonostratigraphy of the Paleoproterozoic Pretoria Group, South Africa. Precambrian Res. 278, 362–393.
Shaanan, U., Rosenbaum, G., Campbell, M.J., 2019. Detrital fingerprint: the use of early Precambrian zircon age spectra as unique identifiers of Phanerozoic terranes. Earth Planet. Sci. Lett. 506, 97–103.
Shannon, R.D., 1976. Revised effective ionic radii and systematic studies of interatomie distances in halides and chalcogenides. Acta Crystallographica A 32, 751–767.
Sircombe, K.N., 2000. Quantitative comparison of large sets of geochronological data using multivariate analysis: a provenance study example from Australia. Geochim. Cosmochim. Acta 64, 1593–1616.
Sircombe, K.N., Stern, R.A., 2002. An investigation of artificial biasing in detrital zircon U-Pb geochronology due to magnetic separation in sample preparation. Geochim. Cosmochim. Acta 66, 2379–2397.
Stacey, J.S., Kramers, J.D., 1975. Approximation of terrestrial lead isotope evolution by a two-stage model. Earth Planet. Sci. Lett. 26, 207–221.
Stern, T.W., Goldich, S.S., Newell, M.F., 1966. Effects of weathering on the U-Pb ages of zircon from the Morton Gneiss, Minnesota. Earth Planet. Sci. Lett. 1, 369–371.
Storey, C.D., Jeffries, T.E., Smith, M., 2006. Common lead-corrected laser ablation ICP–MS U–Pb systematics and geochronology of titanite. Chem. Geol. 227, 37–52.
Tera, F., Wasserburg, G.J., 1972. U-Th-Pb systematics in three Apollo 14 basalts and the problem of initial Pb in lunar rocks. Earth Planet. Sci. Lett. 14, 281–304.
Tilton, G., 1960. Volume diffusion as a mechanism for discordant lead ages. J. Geophys. Res. 65, 2933–2945.
van Niekerk, H.S., 2006. The Origin of the Kheis Terrane and its Relationship with the Archaean Kaapvaal Craton and the Grenvillian Namaqua Province in Southern Africa. Unpublished PhD Thesis. University of Johannesburg 241 pp.
Vermeesch, P., 2013. Multi-sample comparison of detrital age distributions. Chem. Geol. 341, 140–146.
Vermeesch, P., 2018. Dissimilarity measures in detrital geochronology. Earth Sci. Rev. 178, 310–321.
Vorster, C., Kramers, J., Beukes, N., van Niekerk, H., 2016. Detrital zircon U–Pb ages of the Palaeozoic Natal Group and Msikaba Formation, Kwazulu-Natal, South Africa: provenance areas in context of Gondwana. Geol. Mag. 153, 460–486.
Wassermann, L., 2006. All of Nonparametric Statistics. Springer, New York, pp. 442.
Williams, I.S., 1998. U-Th-Pb geochronology by ion microprobe. In: McKibben, M.A., Shanks IIIW.C., Ridley, W.I. (Eds.), Applications of Microanalytical Techniques to Understanding Mineralizing Processes. vol. 7. Reviews in Economic Geology, pp. 1–35.
Williams, I.S., 2001. Response of detrital zircon and monazite, and their U–Pb isotopic systems, to regional metamorphism and host-rock partial melting, Cooma complex, southeastern Australia. Aust. J. Earth Sci. 48, 557–580.
Williams, I.S., Compston, W., Black, L.P., Ireland, T.R., Foster, J.J., 1984. Unsupported radiogenic Pb in zircon: a cause of anomalously high Pb- Pb, U-Pb and Th- Pb ages. Contrib. Mineral. Petrol. 88, 322–327.
Willner, A.P., Sindern, S., Metzger, K., Ermolaeva, T., Kramm, U., Puchkov, V., Kronz, A., 2003. Typology and single grain U/Pb ages of detrital zircons from Proterozoic sandstones in the SW Urals (Russia): early time marks at the eastern margin of Baltica. Precambrian Res. 124, 1–29.
Zeh, A., Ovtcharova, M., Wilson, A.H., Schaltegger, U., 2015. The Bushveld complex was emplaced and cooled in less than one million years – results of zirconology, and geotectonic implications. Earth Planet. Sci. Lett. 418, 103–114.
Zeh, A., Wilson, A.H., Ovtcharova, M., 2016. Source and age of upper Transvaal Supergroup, South Africa: age-Hf isotope record of zircons in Magaliesberg quartzite and Dullstroom lava, and implications for Paleoproterozoic (2.5–2.0 Ga) continent reconstruction. Precambrian Res. 278, 1–21.
Zimmermann, U., 2018. The provenance of selected Neoproterozoic to lower Paleozoic basin successions of Southwest Gondwana: a review and proposal for further research. In: Siegesmund, S., Basei, M.A.S., Oyhantcabal, P., Oriolo, S. (Eds.), Geology of Southwest Gondwana. Regional Geology Reviews. Springer International Publishing AG, pp. 561–591.